THE UNIVERSITY OF OKLAHOMA

GRADUATE COLLEGE

CONCURRENT TWO-PHASE FLOW OF LIQUIDS AND AIR THROUGH INCLINED PIPE

A THESIS

SUBMITTED TO THE GRADUATE FACULTY

in partial fulfillment of the requirements for the

degree of

MASTER OF CHEMICAL ENGINEERING

BY

DON WESLEY GREEN

Norman, Oklahoma

1959

CONCURRENT TWO-PHASE FLOW OF LIQUIDS AND AIR THROUGH INCLINED PIPE

A THESIS

APPROVED FOR THE SCHOOL OF CHEMICAL ENGINEERING

BY

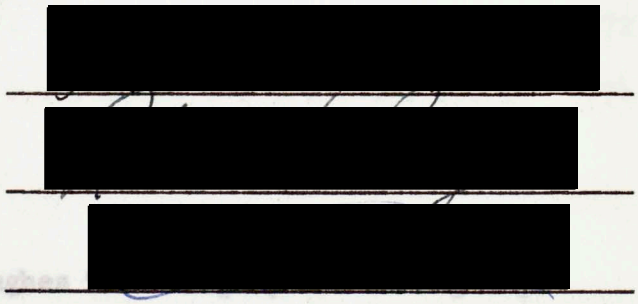

ACKNOWLEDGMENT

The author expresses his appreciation to all those on the University of Oklahoma staff who contributed to this thesis. Particular thanks are extended to:

Dr. R. L. Huntington for his inspiration and guidance throughout the investigation;

The Westcoast Transmission Company, Ltd. and Pacific Petroleums, Ltd. who sponsored this work through a fellowship;

Mr. R. L. Howard for his assistance and suggestions in construction of the equipment;

The following named Chemical Engineering students who assisted in taking data during the experimental program;

Dean Niles

Larry Glasgow

Richard Boyer

Dan Tucker

Eugene Cheatham

Raymond Lohman

Mr. H. L. Baldwin and the Hughes Tool Company for making high speed movies of the two-phase flow.

Don Wesley Green

TABLE OF CONTENTS

LIST OF TABLES

LIST OF ILLUSTRATIONS

CONCURRENT TWO-PHASE FLOW OF LIQUIDS AND AIR THROUGH INCLINED PIPE

CHAPTER I

INTRODUCTION

The concurrent flow of two phases through a pipe has been the object of increased study in recent years as a result of its recognized importance. It is well established that when a liquid phase and a gas phase flow simultaneously through a pipe, the resulting pressure drop is greater than if only a single phase were flowing. Under certain conditions, this "two-phase" pressure drop is further significantly increased when the flow is uphill. Knowledge of gas-liquid two-phase flow is therefore essential to solution of problems arising in such areas as natural gas transmission, oil production gathering systems, heat exchangers, and flow reactors.

In transporting fluids over level terrain, the sound economies of using a single pipe line to carry two phases have been well established in a number of cases. This is seen, for instance, in many of the oil field gathering systems along the Gulf Coast of the United States. However, in hilly country this result may not necessarily hold true. Liquid tends to accumulate in the low places with resulting energy dissipation in "slugging" on the inclines. At low gas rates there may be a slippage of part

of the liquid back down an incline. Energy expended in raising the liquid up a hill is not regained on the downhill side as in single phase flow, which means that each hill is a source of pressure loss even though the ends of the pipe line may be at the same level. Due to these factors, it can be shown that there is an optimum line size for given fluid flow rates up a designated incline. That is, for two-phase flow in hilly country, a pipe line can be oversized just as readily as it can be undersized.

While much experimental work has been conducted in the field of two-phase flow, nearly all design work must still be done using an empirical approach. The problem of measuring factors such as interfacial height and roughness, velocity gradients, and energy expended in transporting and accelerating the liquid phase have made the experimental approach based upon theoretical studies very difficult. A further complication arises from the fact that one or a combination of several distinct types of flow may occur in the two-phase system depending upon such variables as fluid flow rates, fluid physical properties, pipe characteristics, etc.

The major portion of past experimental work has been carried out in horizontal pipe. A lesser number of investigations has been made in vertical pipe, and very few studies made of flow in inclined pipe. Brigham and Holstein[9] observed the flow types and resulting pressure drops occurring at inclines of 5.5° and 12.4° with the horizontal. Flanigan[12] obtained and correlated field data taken from a two-phase pipe line through hilly country, and Baker[3], Berry and Moreau[7] have suggested design procedures to calculate the pressure drop in inclined flow.

This research was undertaken to make an additional study of pressure drops encountered in inclined flow and to compare the results with horizontal two-phase flow, vertical two-phase flow, and other available inclined flow data. Experimental runs were made with the pipe in a horizontal position and at angles of 2.3° and 33° with the horizontal.

It was also felt that data relating the quantity of fluids flowing to the quantity of fluids "in-place" in the pipe would be useful. This was obtained by shutting-in the system and collecting and weighing the liquid in-place in the pipe during a number of designated experimental runs.

As an aid to further qualitative understanding of two-phase flow, the experimental system was made of clear plastic pipe in order that flow patterns could be observed. High speed movies (800 frames/second) and normal speed movies were taken of the flow with the pipe in the horizontal and inclined positions. These movies are available on loan from the School of Chemical Engineering, The University of Oklahoma.

CHAPTER II

PREVIOUS EXPERIMENTAL WORK

One of the earliest important correlations in horizontal two-phase flow was developed by Martinelli, Lockhart[19], et al., at the University of California and presented in final form in 1949. They proposed that there are four basic types of flow:

1. Liquid and gas both in turbulent flow.
2. Liquid flow is viscous and gas flow is turbulent.
3. Liquid flow is turbulent and gas flow is viscous.
4. Liquid and gas both in viscous flow.

The criteria selected for the flow types were a Reynold's Number of 2000 for the gas phase and 1000 for the liquid phase, based upon the total pipe diameter. The correlation for two-phase pressure drop can be expressed mathematically as:

$$\left(\frac{\Delta P}{\Delta L}\right)_{TP} = \phi_l^2 \left(\frac{\Delta P}{\Delta L}\right)_l \qquad (1)$$

$$\left(\frac{\Delta P}{\Delta L}\right)_{TP} = \phi_g^2 \left(\frac{\Delta P}{\Delta L}\right)_g \qquad (2)$$

where;

$$\phi_l^2 = F_1 (X) \qquad (3)$$

$$\phi_g^2 = F_2 (X) \qquad (4)$$

$$X^2 = \left(\frac{\Delta P}{\Delta L}\right)_l \Big/ \left(\frac{\Delta P}{\Delta L}\right)_g \qquad (5)$$

The data are presented graphically with ϕ_l and ϕ_g as a function of X for each of the assumed flow types. Martinelli, et al., were able to correlate their data in this manner to plus 20 or minus 30 per cent.

Several checks on the work of Martinelli and Lockhart have been made with attempts to improve upon the correlation[5,8,11,22]. Gazely and Bergelin[5] at the University of Delaware pointed out that a better test of the data would be a plot of ϕ^2 versus X^2, as $(\Delta P/\Delta L)_g$ appeared in both the abscissa and ordinate. With the more severe test, the data gave maximum deviations of plus 44 and minus 50 per cent. When the data were plotted using the ϕ_l and X parameters, but with constant liquid flow rates, they fell within five per cent of the best line through the points. In addition, these curves had a change of slope which corresponded to an observable change of flow pattern within the pipe. This indicated that within a given Martinelli flow type, such as gas turbulent-liquid turbulent, there were changes of visual flow pattern with resulting quantitative effects on the pressure drop.

Much of the later work has been based on the observable flow pattern changes which occur. Alves[2] made visual studies of co-current liquid-gas flow in a pipe line contactor using clear pipe and described the flow patterns. Considering a pipe initially full of liquid and adding increasing amounts of gas, the successive types of flow to be expected are:

1. Bubble; bubbles of gas having approximately the same velocity as the liquid.

2. Stratified; fluids move in two layers with a smooth interface.

3. Wave; similar to stratified but with gas at a higher velocity

causing waves at interface.

4. Slug; interface level rises and falls, frothy slugs form periodically and move at higher velocities than average liquid velocity.

5. Annular; liquid in moving film on pipe wall with gas traveling at high velocity through central core.

6. Fog or Dispersed; most of liquid occurs as fog entrained within the gas, which is moving at a very high velocity.

Transition between flow types occurs gradually as flow variables are changed. While investigators differ in terminology used and criteria for distinction of the flow, the description by Alves is a good general guide.

Ovid Baker[3] has postulated that the two-phase pressure drop in a horizontal pipe line can be expressed as:

$$\Delta P_{TP} = \Delta P_g \, H \, R \tag{6}$$

where;

H = relative increase in pressure drop due to liquid holdup.

R = relative increase in pressure drop due to wave roughness.

In accordance with this idea, Martinelli's correlation is in effect:

$$\Delta P_{TP} = \Delta P_g \, \phi_g^{\,2} \tag{7}$$

where,

$$\phi_g^{\,2} = HR \tag{8}$$

From laboratory data of Jenkins[17] and Alves[2] in small pipe and field data in eight and ten inch pipe, Baker has determined an empirical equation for ϕ_g for each of the major visual flow patterns. As an example, for slug flow:

$$\phi_g = \frac{1190 \; X^{0.815}}{G_1^{0.5}} \tag{9}$$

These equations are used in conjunction with a flow pattern chart developed by Baker and based on fluid properties as suggested by Holmes[16].

Several investigators at the University of Oklahoma have studied horizontal two-phase flow. A correlation by Schneider[21] involves the use of an "all gas" dimensionless friction factor presented as a function of the dimensionless flow ratio $\frac{G_l \mu_l}{G_g \mu_g}$. The friction factor is defined as:

$$f'_g = \frac{\left(\frac{\Delta P}{\Delta L}\right)_{TP} g \, D \rho_g}{2 G_g^2} \tag{10}$$

Another development was presented by White[24] using a two-phase weighted friction factor plotted as a function of a flow modulus group. These groups are:

$$fw = \frac{2 g_c \, D^6 \, \Delta P_{TP} \, \rho_l}{L \; \frac{W_l^{3.6}}{W_l + W_g}} \tag{11}$$

$$\phi_w = \left(\frac{W_l}{W_g}\right)^{1.8} \left(\frac{\rho_g}{\rho_l}\right)^{.9} \left(\frac{1}{\mu_g \cdot 1}\right) \left(\frac{1}{\mu_l \cdot 1}\right) \tag{12}$$

Data were taken in pipe up to two inches in diameter for both correlations.

A theoretical approach to horizontal two-phase flow was made by Allen[1], considering the flow of a flashing mixture of water and steam. By combining the energy balance equation, momentum balance equation, and equation of continuity, he derived an expression for the ideal case where the water and steam exist as a finely divided mixture with equal average velocities.

Of great interest to the field of horizontal two-phase flow is

the theoretical approach of Gazley[14]. He made experimental studies of stratified flow in two inch pipe to evaluate interfacial stability and energy losses. For liquid flow past stagnant air or gas flow over stagnant liquid, it was found that when the interface was smooth the energy lost by the gas at the interface and that gained by the liquid were approximately equal. At inception of wave flow, the energy lost by the gas was much greater than the energy gained by the liquid, indicating a dissipation of energy in wave formation. This was also found to be true for concurrent flow of the two phases. While the work of Gazley is of very little present practical value since stratified flow rarely occurs, it is a significant contribution in the field of two-phase flow study.

Vertical Flow

Several investigators have experimented with vertical flow. Gosline[15] studied the efficiency of an air lift pump in a glass pipe system which allowed simultaneous study of flow type to be made. Bergelin[6] et al., worked with one inch ID copper tubing to determine the effect of air flow upon pressure drop, with liquid flow rate as a parameter. Poettman and Carpenter[20] studied multiphase flow of gas, oil, and water through vertical flow strings and correlated a modified Reynold's Number against a modified friction factor, based upon the Fanning equation.

At the University of Oklahoma two-phase vertical flow was studied by Galegar, Stovall, and Huntington[13]. In their work, "liquid in-place" data were obtained to determine the effect of fluid flow rates upon slippage of the gas by the liquid. The effect of flow rates on pressure drop was also observed. In the range of flow rates covered, the pressure drop was seen to decline rapidly and tend to a minimum as the air rate was increased at a constant liquid rate.

An early theoretical approach to vertical two-phase flow was made by Versluys[23], in which he considered the flow of gas and crude oil in a producing oil well. He proposed that the principal source of energy came from the expanding of gas within the system and proceeded to derive equations of flow for two cases; (1) gas soluble in the liquid, and (2) gas insoluble in the liquid.

Inclined Flow

While a great deal of work has been done in horizontal and vertical two-phase flow, very few investigators have made studies at intermediate angles of incline. Brigham and Holstein[9] took data in clear plastic test pipe at angles of 5.5° and 12.4° with the horizontal. At low gas rates, slugging occurred which greatly increased the uphill pressure drop as compared with corresponding horizontal values. It was noted that while the system was in slug flow, gas velocity had only a small effect on pressure drop. As gas rate was advanced and flow type moved out of the slug flow region, the inclined pressure drop approached quite closely the horizontal pressure drop for the same fluid rates. They showed that in semi-annular and cresting flow at low angles of incline a horizontal two-phase correlation, such as that of White, was valid.

Flanigan[12] obtained pressure drop values from a two-phase gas-condensate pipe line running through hilly country. He proposed that in inclined flow the total pressure drop could be divided into two components. The first of these was the friction component which occurs in horizontal systems. The second was the liquid head component which appears in uphill flow in addition to the friction component. Flanigan arranged his data and other data from the literature into these two parts

and presented the liquid head effect as a "liquid head factor." This factor is simply the fraction of the total liquid head for the inclines which appears as pressure drop. The values obtained by Flanigan varied from approximately 0.8 at low gas velocities to very nearly zero. Based on the available data it has been suggested by Flanigan[12], Baker[4] and Berry[7] that design calculations for uphill flow be divided into a horizontal calculation and an uphill calculation, with the sum of the pressure drops obtained being used as the overall two-phase effect.

The investigations of two-phase flow discussed give a general view of the type of work that has been conducted in this field. As mentioned, it has been primarily of an empirical nature to enable practical designs to be accomplished. As in all correlations of this type, application to systems different in nature from those in which data were taken must be eyed with caution. At present, the obtaining and correlating of a great deal of data under varied conditions seem to offer the best means of attack on the problem.

CHAPTER III

DESCRIPTION OF APPARATUS

The test section consisted primarily of a loop of 2.12 inch ID clear plastic pipe with dimensions as shown in Figure 1. The pipe was mounted by wiring to an angle iron frame. The frame was held by three supports made from 1-1/2 inch metal pipe fitted inside 2 inch base pipe supports which, in turn, were held by flanges bolted to concrete pads to insure stability. The 1-1/2 inch pipe supports could be set at the desired position by simply bolting them to the 2 inch base pipe. The frame was thus movable to allow the test section pipe to be set at the desired inclination. At the 33° incline position, the high end of the test frame was tied to a metal crosswalk.

The horizontal position of the test section was established by filling the pipe one-half full of water and making necessary leveling adjustments. The inclined positions were set by eye and judged to be no more than plus or minus one inch out of line.

There were two 26 ft. lengths of straight pipe in the test section. The pipe joints were butt joints, glued together with a solution of ethylene dichloride and dissolved pipe shavings. This type of joint was found to be sufficiently strong, easily repaired in case of leaks, and gave a minimum amount of roughness on the inside pipe wall. The loop

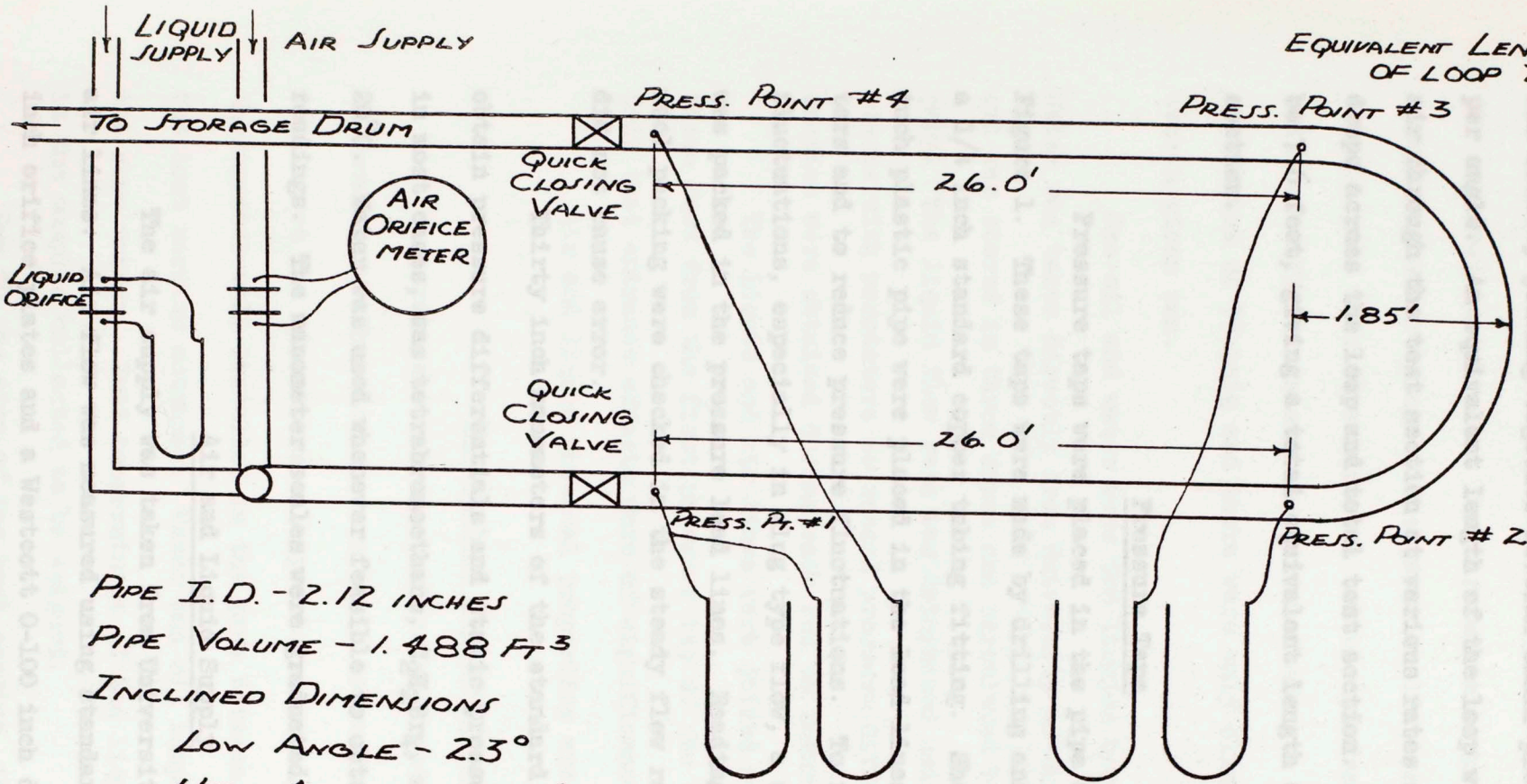

PIPE I.D. - 2.12 INCHES

PIPE VOLUME - 1.488 FT^3

INCLINED DIMENSIONS

LOW ANGLE - 2.3°

HIGH ANGLE - 33.0°

TOTAL RISE

LOW ANGLE - 1.12 FT.

HIGH ANGLE - 15.14 FT.

TOP VIEW - TEST SECTION

FIGURE 1. FLOW DIAGRAM OF APPARATUS

was made by joining together several small pieces of pipe cut at the proper angle. An equivalent length of the loop was determined by flowing air through the test section at various rates and measuring pressure drops across the loop and total test section. This length was found to be 7.6 feet, giving a total equivalent length of 59.6 feet for the test section.

Pressure Taps

Pressure taps were placed in the pipe at four points as shown in Figure 1. These taps were made by drilling and tapping the pipe to fit a 1/4 inch standard copper tubing fitting. Short buffer sections of 1 inch plastic pipe were placed in the lead lines to act as liquid separators and to reduce pressure fluctuations. To further reduce pressure fluctuations, especially in slug type flow, a small amount of glass wool was packed in the pressure lead lines. Readings obtained using glass wool packing were checked in the steady flow range to insure the packing did not cause error.

Thirty inch manometers of the standard "U" tube type were used to obtain pressure differentials and static pressure. The manometer fluid, in most cases, was tetrabromoethane, $C_2H_2Br_4$, with a density of 2.95 at 20°C. Water was used whenever feasible to obtain the lower pressure readings. The manometer scales were graduated to tenths of an inch.

Air and Liquid Supply

The air supply was taken from University of Oklahoma compressed air lines. Air flow was measured using standard flat edge 0.625 and 1.0 inch orifice plates and a Westcott 0-100 inch differential orifice meter.

The orifice plate was mounted in an orifice flange containing flange taps for pressure lead lines. Downstream static pressure was obtained with a Champion pressure gauge. The gauge could be read accurately to the nearest 0.1 psi. Air flow rate was calculated from the meter reading using orifice coefficients and correction factors. The air supply line was at a pressure of 75 psig and there were only slight fluctuations in the flow over a given run.

Gas-oil and water were the liquids used in the experimental runs. Water was taken directly from University of Oklahoma water lines. Gas-oil was stored in three drums and circulated by means of a centrifugal pump. The liquid flow rate was determined using calibrated orifice plates with manometers to record pressure differentials. Weighed liquid samples were obtained during each run to insure accurate measurement.

The liquid and air lines were joined at a cross tee approximately three feet from the first pressure tap of the test section. It is not felt that entrance effects were of significance in the flow range studied.

Air and liquid physical properties are listed in Table 1.

Temperature Measurements

Temperatures were measured using standard 0-120°F. mercurial thermometers. The thermometers could be read accurately to the nearest 1/2 degree F. Air entrance temperatures were measured by means of a thermometer well installed in the pipe between the air orifice plate and the test section entrance. Water and oil temperatures were obtained in the same manner. Exit temperatures of the liquids were measured directly in the samples collected to be weighed.

Due to the size of the test section, it was set up out-of-doors.

TABLE 1

AIR AND LIQUID PHYSICAL PROPERTIES

Component	Density	Viscosity
WATER	62.2 #/ft^3 @ 85°F	1.0 centistokes @ 70°F
GAS-OIL	39.4 °API @ 85°F	3.38 centistokes @ 100°F
AIR	.0808 #/ft^3 @ 32°F 14.7 psia	.018 centipoise @ 80°F

This resulted in a considerable temperature variation from day to day. As the air entered relatively dry, evaporation in the test pipe during water-air runs resulted in a temperature change of the flowing fluids amounting to 7°F or less.

Provision for Shut-In Data

Quick-closing valves were installed at the entrance and exit of the test pipe. These valves were used to obtain "in-place" data. One-half inch drain lines were provided at the entrance and exit to draw off liquid trapped in the pipe after shutting in the system.

To aid in understanding the apparatus, Figure 2 is included to give an overall view of the test section.

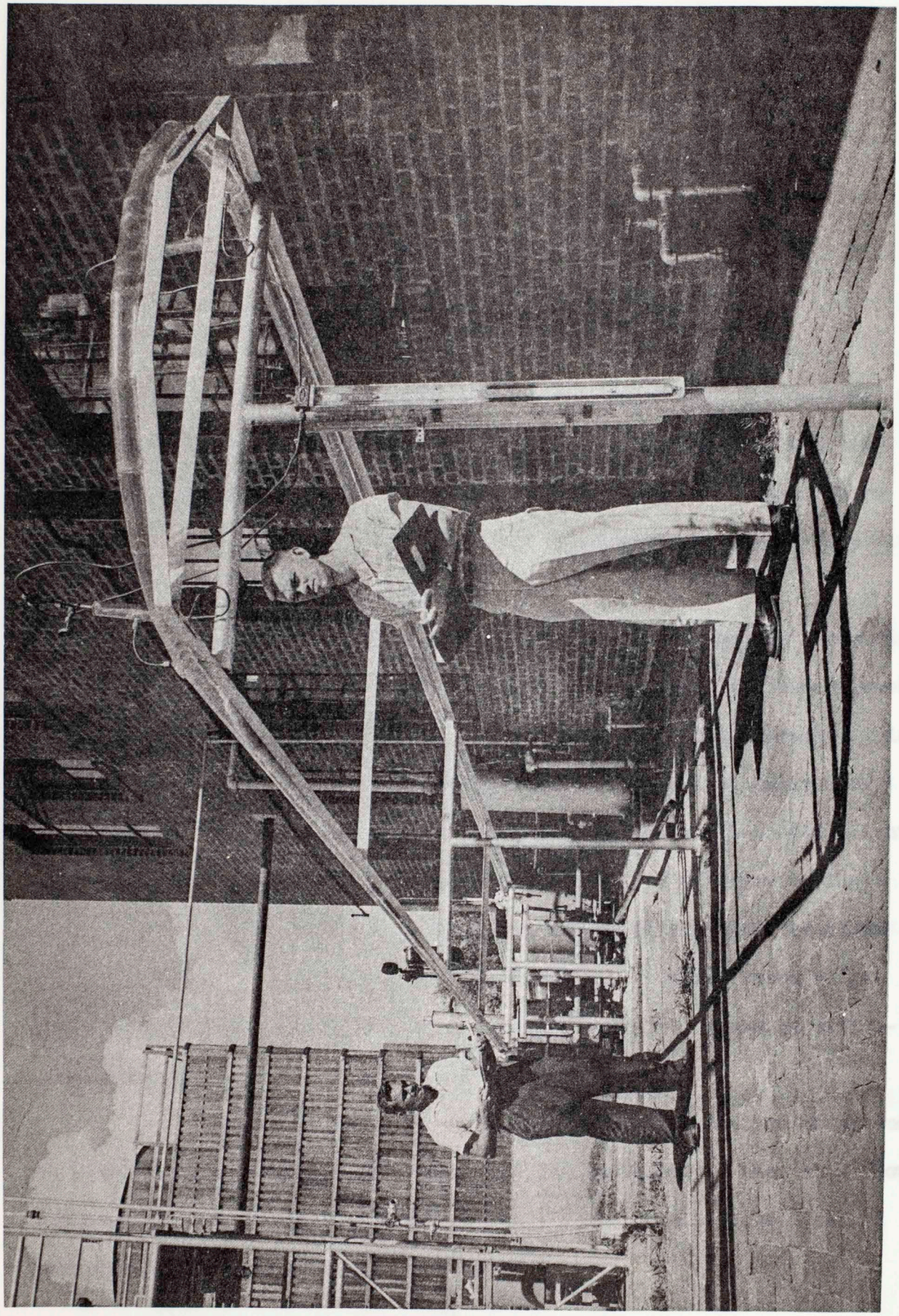

FIGURE 2. PHOTOGRAPH OF TEST SECTION

CHAPTER IV

EXPERIMENTAL PROCEDURE AND DATA

Before beginning the experimental two-phase runs, the orifice meters used to set liquid rates were calibrated by catching timed samples. An equivalent length of the test section loop and pressure drop as a function of air rate were determined by obtaining pressure drop data for various single phase air rates.

The barometric pressure was recorded prior to each day's experimental runs. At the beginning of each run, the air rate was established by setting the desired differential pressure on the orifice meter. This gave an approximate desired air mass velocity only, as the exact flow could not be determined until calculations using the orifice coefficient, pressure, and temperature, were made. Variations in air flow during a given run were very small, and variations in the differential readings were negligible in most cases. At the highest air rates, where slight fluctuations occurred, an average value of the orifice pressure differential was used.

The liquid rate was set by means of the liquid orifice meter and by catching timed samples after the flow had stabilized. When slug flow occurred in the system, two or more timed liquid samples were obtained and an average value used for calculations.

All pressure and temperature readings were recorded after flow had stabilized. The differential pressure across the entire system was obtained from pressure point #1 to pressure point #4. (See Figure 1.) Entrance static pressure was obtained at pressure point #1. In the earlier runs, a loop differential pressure was obtained from pressure point #2 to pressure point #3. In later runs, only static pressure was obtained at point #2 and point #3.

The flow type was next observed and described. This description included a general classification as to type of flow as well as remarks concerning the appearance. During slug flow, the number of slugs per minute was determined. In inclined runs, both uphill and downhill flow types were noted.

For rates in which shut-in data were desired, the experimental run was concluded by simultaneously closing the quick-closing valves at each end of the test section. This operation required two men. One man closed the two valves at a predetermined signal while a second man shut in the air and liquid supplies. After this shut-in operation, liquid in the test section was drained through the two drain lines provided for 3 to 5 minutes. No attempt was made to remove the small amount of liquid which remained on the pipe walls after draining.

Experimental Data

Experimental runs were made at the following liquid mass velocities:

3,370 #/hr-ft^2	(Gas-Oil only)
13,750 #/hr-ft^2	
28,800 #/hr-ft^2	
66,100 #/hr-ft^2	
90,000 #/hr-ft^2	(Gas-Oil only)
110,000 #/hr-ft^2	(Water only)

At each of these liquid rates, the air mass velocity was varied between 3,500 #/hr-ft^2 and 23,000 #/hr-ft^2. These combinations were followed with the pipe in a horizontal position and at inclines of 2.3° and 33°. All liquid and air mass velocity values are based upon the total pipe cross sectional area.

Two-phase data taken are listed in Tables 2 - 7. The runs at a constant liquid rate are grouped in each table. Pressures listed are an average static pressure over the test section. Air temperatures recorded are those obtained at the entrance thermometer well. Pressure drop data are the total pressure drops over the test section divided by the equivalent length of the test section.

Single phase air pressure drop data are shown in Table 8. Calculated values of the Moody friction factor are also included.

Values of the calculated White correlation functions for the 'gas-oil'-air system are tabulated in Tables 9 and 10 for the horizontal and 33° incline positions respectively.

Experimental Error

The greatest error in reading static and differential pressures occurred in slug type flow. In a few instances, average fluctuations were as much as 50 to 100 per cent of the total reading, but in most cases, they were on the order of 25 to 50 per cent of the total reading. In all runs, an attempt was made to obtain an average reading. At least two independent readings were made where violent fluctuations occurred. Based on the average fluctuation in slug flow, it is felt the data are accurate to within plus or minus 15 per cent. In other types of flow, the readings are believed to be accurate to plus or minus 5 per cent.

All slug flow data points are so indicated in the data tables.

Liquid flow rates are judged to be accurate to plus or minus 5 per cent in all types of flow except slug flow, where the rates are accurate to within plus or minus 10 per cent. Air rates are thought to be accurate to within plus or minus 5 per cent.

Temperatures taken at entrance thermometer wells are believed to be within 1°F. of actual values. In water-air runs, evaporation within the system resulted in a liquid and air temperature change. The resulting error in calculations is less than 2 per cent.

Results of checking the data against the White correlation indicate that actual errors are within the limits as stated.

In obtaining shut-in data, no extensive effort was made to clean the test section of all the trapped liquid. The pipe was allowed to drain for 3 to 5 minutes after the test section was closed in. There would be an error resulting from the inability of the operator to close the quick-closing valves simultaneously. Here again, the greatest error occurs in slug flow, as the flow pattern is unstable.

TABLE 2

EXPERIMENTAL DATA

Angle of Incline - 0°

Test Fluids - Air, Water

Run No.	G_l #/Hr-Ft^2	G_{Air} #/Hr-Ft^2	T_{Air} °R	T_l °R	P_{avg} #/In^2	$\Delta P/L$ #/Ft^2-Ft	SIR Ft^{3}Air/ Ft^{3}Liq	FR Ft^{3}Air/ Ft^{3}Liq	Flow Type
229	13,750	3,370	552	546	14.16	.051	--	--	R *
20	13,750	5,070	552	551	14.14	.077	--	--	R
230	14,050	6,570	550	547	14.19	.18	--	--	R
6	14,050	9,000	528	523	14.34	.307	--	--	R
235	14,050	10,600	551	542	14.65	.425	--	--	W
7	14,050	13,380	530	523	14.45	.748	--	--	W
21	14,050	14,610	549	539	14.36	.836	--	--	W
8	14,050	17,420	529	523	14.63	1.19	--	--	W
9	14,050	23,500	530	523	14.94	2.06	--	--	SA
231	28,800	3,650	553	547	14.17	.077	--	--	R
162	28,800	5,020	558	549	14.13	.129	--	--	R
232	28,500	6,690	547	544	14.21	.232	--	--	W
154	29,100	8,750	556	548	14.25	.411	--	--	W
236	28,800	10,600	550	543	14.32	.565	--	--	W
155	28,800	13,020	556	548	14.39	.864	--	--	W
156	28,800	17,050	555	548	14.48	1.43	--	--	W
157	29,100	22,800	553	548	14.97	2.59	--	--	W
301	66,100	3,340	545	541	14.13	.206	--	--	W-S
19	66,600	5,080	553	551	14.20	.232	4.99	68.9	S
234	66,100	6,600	551	542	14.26	.386	6.05	89.0	W

* See Table 11 for Flow Type Nomenclature.

TABLE 2 (Continued)

Run No.	G_l #/Hr-Ft^2	G_{Air} #/Hr-Ft^2	T_{Air} °R	T_l °R	P_{avg} #/In^2	$\Delta P/L$ #/Ft^2-Ft	SIR Ft^{3}Air/ Ft^{3}Liq	FR Ft^{3}Air/ Ft^{3}Liq	Flow Type
10	66,100	9,390	532	523	14.48	.697	--	--	W
237	67,000	10,650	549	543	14.42	.912	--	--	W
302	65,600	10,800	540	540	14.33	.875	--	--	W
12	66,100	13,200	536	533	14.52	1.63	15.5	170	W
22	66,100	12,730	547	540	14.48	1.16	--	--	W
242	66,100	13,300	540	540	14.49	1.24	--	--	W-C
11	66,100	17,400	536	533	14.94	2.11	--	--	SA-C
13	66,100	23,950	536	532	15.59	3.77	19.9	287	SA
300	110,000	3,640	545	541	14.19	.334	--	--	S
18	110,000	5,150	546	544	14.33	.413	4.38	41.0	S
228	109,000	6,610	546	542	14.27	.541	4.77	53.6	C
17	110,000	8,910	546	544	14.39	.928	--	--	W-S
238	109,500	10,600	549	543	14.46	1.16	7.40	84.9	C
15	110,000	13,100	539	531	14.79	1.73	--	--	C
243	110,500	14,600	540	541	14.87	2.16	--	--	C
16	110,000	17,550	544	544	15.22	2.84	--	--	SA
14	110,000	23,800	537	532	16.04	4.72	13.8	167	SA

TABLE 3

EXPERIMENTAL DATA

Angle of Incline - 0°

Test Fluids - Air, Gas-Oil

Run No.	G_l #/Hr-Ft^2	G_{Air} #/Hr-Ft^2	T_{Air} °R	T_l °R	P_{avg} #/In^2	$\Delta P/L$ #/Ft^2-Ft	SIR Ft^{3}Air/ Ft^{3}Liq	FR Ft^{3}Air/ Ft^{3}Liq	Flow Type
270	3,370	3,580	537	542	14.14	.050	--	--	R
269	3,370	4,900	535	541	14.16	.085	--	--	W-R
268	3,370	6,560	533	541	14.18	.139	--	--	W
264	3,370	8,890	539	543	14.21	.250	--	--	W
265	3,370	10,900	539	543	14.24	.360	--	--	W
266	3,370	13,400	540	545	14.29	.522	--	--	W
267	3,370	17,280	539	545	14.46	.867	--	--	W
252	13,750	3,500	544	549	14.14	.058	5.13	188	R
253	13,750	3,590	538	538	14.15	.068	--	--	R
44	13,750	5,200	556	565	14.14	.129	7.35	284	R
254	13,750	6,590	538	540	14.18	.216	--	--	W
50	13,750	8,750	556	567	14.20	.360	11.2	348	W
251	14,350	10,720	546	548	14.23	.475	23.0	548	W
51	13,750	12,930	557	568	14.32	.696	--	--	SA
52	13,750	17,030	555	566	14.49	1.24	37.3	911	SA
53	13,750	22,600	553	566	14.79	2.17	--	--	SA
255	28,800	3,550	542	540	14.15	.100	3.33	90.0	W
163	28,800	4,960	561	551	14.15	.180	--	--	W
256	28,800	6,680	539	542	14.21	.272	7.29	168	W
158	28,800	8,800	558	553	14.27	.450	--	--	W-SA
250	29,100	10,700	542	545	14.33	.618	13.6	265	W-SA
159	29,100	13,020	557	552	14.43	.941	--	--	SA

TABLE 3 (Continued)

Run No.	G_l #/Hr-Ft^2	G_{Air} #/Hr-Ft^2	T_{Air} °R	T_l °R	P_{avg} #/In^2	$\Delta P/L$ #/Ft^2-Ft	SIR Ft^{3}Air/ Ft^{3}Liq	FR Ft^{3}Air/ Ft^{3}Liq	Flow Type
160	29,100	17,100	555	552	14.65	1.57	25.1	424	SA
161	29,100	22,600	553	553	15.09	2.81	--	--	SA
257	66,100	3,480	538	541	14.16	.157	3.04	38.2	S
259	66,100	5,040	538	542	14.20	.296	3.45	55.0	W
260	66,100	6,700	539	543	14.25	.450	4.77	72.5	W
262	66,100	8,960	539	545	14.36	.746	--	--	SA
247	66,100	11,000	539	541	14.48	1.09	8.37	118	SA
263	66,100	13,500	539	545	14.62	1.53	--	--	SA
248	66,600	17,550	540	542	14.92	2.33	14.6	183	SA
249	66,600	23,700	540	543	15.54	3.94	20.2	236	SA
284	67,000	23,700	543	550	15.47	3.96	--	--	SA
258	90,000	3,540	537	542	14.17	.261	3.51	28.6	S
45	90,000	4,970	555	562	14.21	.360	3.58	41.1	S
261	90,000	6,675	539	543	14.24	.643	4.53	53.3	SA-S
46	90,000	8,750	559	567	14.33	.928	--	--	C
245	90,500	10,640	539	540	14.60	1.31	--	--	SA-C
47	90,000	13,230	552	563	14.68	1.78	8.45	106	SA
48	90,000	17,550	552	563	15.06	2.85	--	--	SA
246	90,000	17,950	538	540	15.13	2.92	--	--	SA
49	90,000	23,600	549	563	15.69	4.45	18.2	175	SA

TABLE 4

EXPERIMENTAL DATA

Angle of Incline - 2.3°

Test Fluids - Air, Water

Run No.	G_l #/Hr-Ft^2	G_{Air} #/Hr-Ft^2	T_{Air} °R	T_l °R	P_{avg} #/In^2	$\Delta P/L$ #/Ft^2-Ft	SIR Ft^{3}Air/ Ft^{3}Liq	FR Ft^{3}Air/ Ft^{3}Liq	Flow Type Rise/Fall	
291	14,050	3,520	543	542	14.13	1.80	10.2	232	S	W
32	13,750	4,850	555	548	14.15	.206	--	--	S	W
219	14,050	6,550	551	548	14.20	.282	12.2	418	W	W
23	13,750	8,920	553	541	14.21	.348	--	--	W	W
240	13,500	10,500	551	541	14.28	.464	32.7	690	W	W
24	13,750	13,180	549	546	14.32	.682	--	--	W	W
304	13,750	13,380	540	538	14.28	.713	--	--	W	W
25	13,750	16,970	546	541	14.46	1.12	--	--	W	W
303	13,750	17,100	540	541	14.42	1.15	--	--	W	W
292	28,200	3,630	543	542	14.13	.266	--	--	S	W
293	29,100	5,100	542	542	14.13	.283	--	--	S	W
222	28,500	6,590	544	542	14.23	.348	--	--	S	W
150	28,200	8,800	553	544	14.23	.449	--	--	W	W
241	29,100	10,650	551	541	14.33	.618	--	--	W	W
151	28,800	12,900	556	544	14.40	.890	--	--	W	W
152	28,800	17,100	554	544	14.62	1.47	--	--	W	W
153	28,800	22,800	551	544	15.03	2.61	--	--	W	W
294	66,100	3,380	543	541	14.11	.360	5.36	8.61	S	W
295	66,600	5,080	543	541	14.19	.437	6.16	10.91	S	W
296	66,100	6,650	541	543	14.26	.565	--	--	S	W
196	66,100	8,700	548	546	14.29	.669	--	--	SA	W

TABLE 4 (Continued)

Run No.	G_l #/Hr-Ft^2	G_{Air} #/Hr-Ft^2	T_{Air} °R	T_l °R	P_{avg} #/In^2	$\Delta P/L$ #/Ft^2-Ft	SIR Ft^{3}Air/ Ft^{3}Liq	FR Ft^{3}Air/ Ft^{3}Liq	Flow Rise/Fall	Type
197	66,600	10,980	548	546	14.41	.940	10.7	144	SA	W
198	66,100	13,100	548	549	14.49	1.246	12.61	172	SA	W
199	66,100	17,400	547	539	14.78	2.005	16.05	224	SA	SA
289	66,100	17,450	538	539	14.81	2.130	--	--	SA	SA
200	66,100	23,500	547	539	15.43	3.70	20.5	289	SA	SA
298	110,000	3,640	544	541	14.27	.515	4.7	29.0	S	W
297	110,000	5,110	543	541	14.25	.616	4.82	40.2	S	W
299	110,000	6,690	543	541	14.32	.770	5.76	52.6	S	C
27	110,000	8,900	551	545	14.41	.979	--	--	S	C
28	110,000	11,200	550	544	14.60	1.440	8.05	87.8	S	C
239	110,500	13,250	551	541	14.63	1.722	9.24	104	S-C	C
290	109,500	13,350	539	539	14.72	1.803	--	--	S-C	C
29	110,000	17,520	548	541	15.08	2.940	--	--	C	C
30	110,000	22,100	548	539	15.65	4.195	13.28	161.5	SA	SA
26	13,750	22,950	545	540	14.75	1.96	--	--	W	W

TABLE 5

EXPERIMENTAL DATA

Angle of Incline - 2.3°

Test Fluids - Air, Gas-Oil

Run No.	G_l #/Hr-Ft^2	G_{Air} #/Hr-Ft^2	T_{Air} °R	T_l °R	P_{avg} #/In^2	$\Delta P/L$ #/Ft^2-Ft	SIR Ft^{3}Air/Ft^{3}Liq	FR Ft^{3}Air/Ft^{3}Liq	Flow Type Rise/Fall
271	3,370	3,330	536	545	14.13	.166	--	--	S W
272	3,370	5,110	536	545	14.16	.210	--	--	S W
273	3,370	6,660	538	548	14.17	.244	--	--	W R
285	3,370	8,850	543	553	14.19	.276	--	--	W W
286	3,370	10,700	544	555	14.21	.366	--	--	W W
287	3,370	13,000	543	555	14.32	.526	--	--	W W
288	3,370	17,100	543	556	14.38	.875	--	--	W W
213	13,750	3,430	548	548	14.14	--	8.17	185	S W
274	13,750	3,345	542	543	14.17	.174	--	--	S W
33	13,750	5,040	556	564	14.16	.259	--	--	S W
214	13,750	6,620	548	549	14.19	.309	10.3	349	W W
35	13,750	8,750	559	567	14.22	.387	16.8	473	W W
202	14,050	10,750	539	538	14.28	.502	21.4	552	SA W
36	13,750	12,970	557	566	14.33	.748	--	--	SA SA
37	13,750	16,860	556	565	14.50	1.24	35.0	896	SA SA
38	13,750	23,000	552	565	14.82	2.24	--	--	SA SA
275	28,800	3,590	541	545	14.16	.218	--	--	S W
305	29,100	5,130	544	549	14.13	.309	--	--	S W
276	28,800	5,070	542	545	14.17	.288	--	--	S W
277	28,500	6,700	540	547	14.21	.418	--	--	S W
306	28,500	6,770	544	549	14.18	.399	--	--	SA-S W
146	28,800	8,840	553	551	14.27	.488	--	--	SA W

TABLE 5 (Continued)

Run No.	G_l #/Hr-Ft^2	G_{Air} #/Hr-Ft^2	T_{Air} °R	T_l °R	P_{avg} #/In^2	$\Delta P/L$ #/Ft^2-Ft	SIR Ft^{3}Air/ Ft^{3}Liq	FR Ft^{3}Air/ Ft^{3}Liq	Flow Type Rise/Fall	
201	28,800	10,670	539	538	14.33	.669	--	--	SA	W
147	28,500	13,100	553	551	14.44	.952	--	--	SA	SA
148	28,800	17,350	551	555	14.68	1.66	--	--	SA	SA
149	29,100	22,600	550	555	15.07	2.83	--	--	SA	SA
278	66,600	3,540	542	547	14.15	.401	--	--	S	W
209	65,600	3,580	543	543	14.20	--	4.90	39.8	S	W
210	65,600	4,910	544	544	14.22	--	5.08	54.5	S	W
307	66,100	5,010	546	549	14.20	.515	--	--	S	W
215	66,100	6,650	547	550	14.27	--	6.58	73.8	W	W
308	65,600	6,650	544	549	14.23	.642	--	--	S	W
203	66,600	8,730	541	538	14.27	.823	--	--	SA-S	SA-C
204	65,600	10,900	541	539	14.43	1.16	8.36	119	SA-C	SA-C
205	66,100	13,300	541	541	14.63	1.57	--	--	SA-C	SA-C
206	66,600	17,450	540	541	14.9	2.42	14.4	181	SA	SA
283	67,000	23,700	541	549	15.48	3.94	--	--	SA	SA
207	66,100	22,800	539	542	15.35	3.58	19.1	231	SA	SA
279	89,200	3,460	548	548	14.19	.523	--	--	S	W
216	90,000	3,450	550	550	14.18	--	4.63	28.5	S	W
280	89,200	5,110	548	548	14.23	.661	--	--	S	W
43	90,000	5,090	548	545	14.27	.515	4.83	41.5	S	W
281	89,500	6,740	548	548	14.26	.838	--	--	SA-S	W
217	90,000	6,590	549	550	14.29	--	5.53	53.9	SA-S	W
42	90,000	8,910	548	557	14.48	1.13	--	--	S	S-C
208	90,500	10,930	541	543	14.54	1.39	7.35	85.8	SA-S	SA-C
40	90,000	12,480	551	549	14.70	1.75	7.90	97.8	SA-C	SA
282	90,000	17,650	543	549	15.06	2.83	--	--	SA	SA
41	90,000	17,250	548	557	15.08	2.78	--	--	SA	SA
39	90,000	23,500	544	547	15.63	4.43	15.8	174	SA	SA

TABLE 6

EXPERIMENTAL DATA

Angle of Incline - 33°

Test Fluids - Air, Water

Run No.	G_l #/Hr-Ft^2	G_{Air} #/Hr-Ft^2	T_{Air} °R	T_1 °R	P_{avg} #/In^2	$\Delta P/L$ #/Ft^2-Ft	SIR Ft^3/Air/ Ft^{3}liq	FR Ft^{3}Air/ Ft^{3}Liq	Flow Type Rise/Fall
404	14,050	3,760	526	529	14.86	2.98	9.08	218	S W
405	13,750	5,425	527	529	14.73	2.44	11.7	324	S W
406	14,050	6,850	524	526	14.70	2.32	12.6	399	S W
366	13,750	9,600	510	513	14.76	2.24	15.5	555	S-SA W
367	14,050	11,150	511	513	14.73	2.15	18.8	636	S-SA W
368	13,750	12,570	513	513	14.74	2.11	--	--	S-SA W
369	13,750	13,830	515	513	14.77	2.11	21.5	806	S-SA W
370	13,750	15,550	516	513	14.79	2.06	--	--	S-SA W
371	13,450	17,880	516	513	14.78	1.90	28.0	1,070	SA-C W
372	13,750	20,050	517	513	14.83	1.85	--	--	SA W
373	13,750	23,500	519	513	14.94	2.06	--	--	SA W
407	29,100	3,765	524	525	14.61	2.75	--	--	S W
408	29,100	5,275	524	524	14.53	2.68	--	--	S W
409	29,400	6,940	524	524	14.56	2.55	--	--	S W
374	28,800	9,480	513	509	14.78	2.54	--	--	S-SA W
375	28,800	11,060	514	510	14.78	2.54	--	--	S-SA W
376	28,800	12,980	515	510	14.82	2.49	--	--	S-SA W
377	28,800	14,700	516	510	14.82	2.44	--	--	S-SA W
378	28,800	17,200	517	511	14.87	2.49	--	--	SA-C W
379	28,800	20,600	518	513	14.97	2.60	--	--	SA W
382	28,800	22,030	520	513	15.04	2.65	--	--	SA SA
380	28,800	23,700	520	513	15.19	2.96	--	--	SA SA

TABLE 6 (Continued)

Run No.	G_l #/Hr-Ft^2	G_{Air} #/Hr-Ft^2	T_{Air} °R	T_l °R	P_{avg} #/In^2	$\Delta P/L$ #/Ft^2-Ft	SIR Ft^{3}Air/ Ft^{3}Liq	FR Ft^{3}Air/ Ft^{3}Liq	Flow Type Rise/Fall
381	28,800	25,300	521	513	15.30	3.22	--	--	SA SA
398	66,100	3,640	519	509	14.98	3.83	6.65	43.8	S W
399	66,100	5,350	519	509	14.80	3.50	7.58	65.0	S W
400	67,000	6,950	519	509	14.83	3.39	9.85	83.3	S W
383	66,100	9,240	517	521	14.98	3.37	10.3	111	S W
384	66,100	11,430	517	520	14.99	3.27	11.2	137	S W
385	66,600	12,500	517	519	15.10	3.32	--	--	S-SA W
386	66,100	13,720	517	518	15.11	3.47	12.0	163	S-SA W
387	66,100	16,100	518	516	15.16	3.55	--	--	S-SA W
388	66,600	18,400	519	515	15.29	3.73	14.2	216	S-SA W
390	66,100	21,000	520	515	15.39	3.78	--	--	S-SA W
389	66,100	24,400	520	515	15.74	4.55	--	--	SA-C W
401	109,000	3,765	523	529	15.06	4.14	--	--	S W
402	110,000	5,400	524	528	15.11	3.92	--	--	S W
403	110,000	7,090	524	527	15.12	3.66	--	--	S W
391	110,000	9,560	511	510	14.94	3.78	--	--	S W
392	109,000	11,540	514	510	15.10	3.96	--	--	S-SA W
393	110,000	14,250	515	509	15.34	4.22	--	--	S-SA W
394	110,000	15,900	516	509	15.30	4.43	--	--	S-SA W
395	110,000	18,570	518	509	15.57	4.78	--	--	S-SA W
397	110,000	21,200	519	509	15.74	5.15	--	--	S-SA W
396	110,000	25,050	518	509	16.15	5.96	--	--	S-SA-C SA

TABLE 7

EXPERIMENTAL DATA

Angle of Incline - 33°

Test Fluids - Air, Gas-Oil

Run No.	G_l #/Hr-Ft^2	G_{Air} #/Hr-Ft^2	T_{Air} °R	T_l °R	P_{avg} #/In^2	$\Delta P/L$ #/Ft^2-Ft	SIR Ft^{3}Air/ Ft^{3}Liq	FR Ft^{3}Air/ Ft^{3}Liq	Flow Type Rise/Fall
309	3,370	3,630	535	540	14.57	2.24	--	--	S W
310	3,370	5,170	532	541	14.51	1.93	--	--	S W
311	3,370	6,730	532	542	14.48	1.73	--	--	S W
312	3,370	9,130	534	543	14.45	1.52	--	--	S-SA W
313	3,370	10,970	534	544	14.41	1.27	--	--	S-SA W
319	3,370	12,050	532	538	14.31	.824	--	--	SA-C W
314	3,370	13,400	534	544	14.30	.707	--	--	SA W
318	3,370	14,800	538	545	14.33	.771	--	--	SA W
315	3,370	17,300	535	544	14.40	.963	--	--	SA W
317	3,370	19,600	537	545	14.48	1.18	--	--	SA W
316	3,370	23,000	535	544	14.65	1.68	--	--	SA SA
350	13,750	3,590	529	536	14.68	2.19	9.87	180	S W
351	13,750	5,120	530	536	14.65	2.01	14.8	332	S W
352	14,350	6,890	531	536	14.65	1.90	--	--	S W
320	13,750	9,260	536	537	14.51	1.85	16.2	474	S-SA W
321	14,050	11,000	535	540	14.52	1.76	19.1	550	S-SA W
325	13,750	12,450	514	516	14.92	1.70	--	--	S-SA W
322	13,750	13,400	534	541	14.49	1.58	23.5	686	SA-S-C W
326	13,750	15,500	516	516	14.72	1.47	--	--	SA-S-C W
323	13,750	17,300	534	541	14.59	1.66	31.4	875	SA-C W
327	13,750	20,300	517	517	14.91	1.86	--	--	SA SA
324	13,750	22,900	534	541	14.87	2.24	42.9	1,140	SA SA

TABLE 7 (Continued)

Run No.	G_l #/Hr-Ft^2	G_{Air} #/Hr-Ft^2	T_{Air} °R	T_l °R	P_{avg} #/In^2	$\Delta P/L$ #/Ft^2-Ft	SIR Ft^{3}Air/ Ft^{3}Liq	FR Ft^{3}Air/ Ft^{3}Liq	Flow Type Rise/Fall
347	28,800	3,780	525	529	14.71	2.57	8.88	89.3	S W
348	29,100	5,320	526	530	14.67	2.26	10.1	13.3	S W
349	29,400	6,890	528	533	14.65	2.16	12.5	162	S W
344	28,500	9,230	536	539	14.56	2.11	15.8	226	S W
335	28,800	10,900	536	542	14.55	1.98	15.2	265	S-SA W
328	28,800	12,350	539	544	14.81	2.14	--	--	S-SA W
336	29,100	13,700	535	543	14.67	2.24	17.9	330	S-SA SA
329	28,800	15,450	537	544	14.93	2.26	--	--	S-SA SA
337	28,800	17,600	535	543	14.81	2.65	20.9	420	SA-C SA
330	28,800	20,600	536	544	15.19	2.84	--	--	SA-C SA
338	28,800	23,700	540	547	15.24	3.56	28.9	555	SA SA
344	66,600	3,570	534	537	14.89	3.06	6.75	36.7	S W
345	67,000	4,980	534	537	14.88	2.98	--	--	S W
346	66,600	6,880	533	537	14.86	2.91	10.4	70.7	S W
339	66,100	9,150	541	547	14.63	2.44	10.6	98.0	S W
340	66,600	10,950	539	546	14.72	2.52	11.3	112	S-SA SA
331	67,400	12,350	538	545	15.00	2.68	--	--	S-SA SA
341	66,600	13,600	539	546	14.75	2.98	--	--	S-SA SA
342	66,600	18,200	537	543	15.19	3.78	14.2	185	S-SA SA
333	66,600	20,800	537	543	15.67	4.31	--	--	SA-S-C SA
343	66,600	24,000	534	537	15.89	5.05	17.9	250	S W
353	89,200	3,820	524	527	14.92	3.29	--	--	S W
354	89,200	5,400	524	527	14.90	3.01	--	--	S W
355	90,000	7,100	530	528	14.87	2.80	--	--	S W
356	90,000	9,050	528	530	14.93	2.70	--	--	S W
357	90,000	11,450	528	530	14.99	2.86	--	--	S-SA SA
359	90,000	12,500	529	531	15.04	2.98	--	--	S-SA SA
358	90,000	13,850	529	530	15.09	3.14	--	--	S-SA SA
360	90,000	15,600	529	532	15.17	3.30	--	--	S-SA SA
361	90,000	18,000	530	532	15.35	3.60	--	--	SA-C SA

TABLE 8

EXPERIMENTAL DATA

Single Phase Air Flow

Run No.	G_{Air} #/hr-ft^2	T_{Air} °R	P_{avg} #/in^2	$\Delta P/L$ #/ft^3-ft	fm	Re
A	5,740	553	14.02	.0772	.0237	2.30×10^4
B	8,120	553	14.04	.167	.0257	3.24×10^4
C	10,000	553	14.06	.244	.0249	3.99×10^4
D	11,580	553	14.08	.309	.0235	4.62×10^4
E	13,170	553	14.10	.398	.0234	5.25×10^4
F	14,300	553	14.12	.475	.0236	5.71×10^4
G	15,500	553	14.14	.552	.0235	6.19×10^4
H	16,500	553	14.16	.618	.0232	6.59×10^4
I	17,550	553	14.19	.695	.0231	7.00×10^4
J	6,670	549	14.16	.109	.0249	2.67×10^4
K	5,180	549	14.15	.0676	.0256	2.08×10^4
L	3,590	548	14.14	.0372	.0294	1.44×10^4

TABLE 9

WHITE CORRELATION

Coordinates for Figure 13

Angle of Incline - 0°

Test Fluids - Air, Gas-Oil

Run No.	G_l #/Hr-Ft^2	G_{Air} #/Hr-Ft^2	ϕ_w	f_w
270	3,370	3,580	.00266	1.41
269	3,370	4,900	.00152	2.84
268	3,370	6,560	.00090	5.58
264	3,370	8,890	.00049	12.4
265	3,370	10,900	.00036	20.6
266	3,370	13,400	.00026	35.4
267	3,370	17,280	.00016	72.2
252	13,750	3,500	.0356	.0254
253	13,750	3,590	.0332	.0300
44	13,750	5,200	.0172	.0623
254	14,750	6,590	.0112	.112
50	13,750	8,750	.00680	.207
251	14,350	10,720	.00501	.261
51	13,750	12,930	.00336	.475
52	13,750	17,030	.00207	.966
53	13,750	22,600	.00128	2.01
255	28,800	3,550	.127	.00579
163	28,800	4,960	.0673	.0109
256	28,800	6,680	.0408	.0173
158	28,800	8,800	.0242	.0303
250	29,100	10,700	.0176	.0422
159	29,100	13,020	.0121	.0684
160	29,100	17,100	.00770	.125
161	29,100	22,600	.00475	.249
257	66,100	3,480	.594	.00098
259	66,100	5,040	.302	.00189
260	66,100	6,700	.183	.00293
262	66,100	8,960	.109	.00502
247	66,100	11,000	.0760	.00754
263	66,100	13,500	.0538	.0109
248	66,600	17,550	.0339	.0171
249	66,600	23,700	.0204	.0312
284	67,000	23,700	.0204	.0308

TABLE 9 (Continued)

Run No.	G_l #/Hr-Ft^2	G_{Air} #/Hr-Ft^2	ϕ_w	f_w
258	90,000	3,540	1.01	.00072
45	90,000	4,970	.560	.00101
261	90,000	6,675	.315	.00183
46	90,000	8,750	.200	.00270
245	90,500	10,640	.143	.00382
47	90,000	13,230	.0985	.00541
48	90,000	17,550	.0615	.00905
246	90,000	17,950	.0578	.00930
49	90,000	23,600	.0372	.0155

$$f_w = \frac{2g_c \; D^6 \; \Delta P_{TP} \; \rho_l}{L \; \dfrac{W_l^{3.6}}{W_l + W_g}}$$

$$\phi_w = \left(\frac{W_l}{W_g}\right)^{1.8} \left(\frac{\rho_g}{\rho_l}\right)^{.9} \left(\frac{1}{\mu_g^{.1}}\right) \left(\frac{1}{\mu_l^{.1}}\right)$$

TABLE 10

WHITE CORRELATION

Coordinates for Figure 14

Angle of Incline - 33°

Test Fluids - Air, Gas-Oil

Run No.	G_l #/Hr-Ft^2	G_{Air} #/Hr-Ft^2	ϕ_w	f_w
309	3,370	3,630	.00259	63.5
310	3,370	5,170	.00142	66.7
311	3,370	6,730	.000883	70.5
312	3,370	9,130	.000505	77.0
313	3,370	10,970	.000362	74.0
319	3,370	12,050	.000306	51.4
314	3,370	13,400	.000250	48.1
318	3,370	14,800	.000211	56.7
315	3,370	17,300	.000162	80.5
317	3,370	19,600	.000128	112
350	13,750	3,590	.0348	.969
351	13,750	5,120	.0185	.965
352	14,350	6,890	.0117	.884
320	13,750	9,260	.00621	1.09
321	14,050	11,000	.00478	1.05
325	13,750	12,450	.00383	1.13
322	13,750	13,400	.00320	1.10
326	13,750	15,500	.00254	1.10
323	13,750	17,300	.00204	1.32
327	13,750	20,300	.00159	1.62
324	13,750	22,900	.00124	2.09
347	28,800	3,780	.121	.150
348	29,100	5,320	.0664	.134
349	29,400	6,890	.0421	.130
334	28,500	9,230	.0234	.147
335	28,800	10,900	.0176	.141
328	28,800	12,350	.0142	.157
336	29,100	13,700	.0119	.165
329	28,800	15,450	.00961	.179
337	28,800	17,600	.00757	.220
330	28,800	20,600	.00581	.252
338	28,800	23,700	.00450	.335
344	66,600	3,570	.602	.0188
345	67,000	4,980	.335	.0184
346	66,600	6,880	.186	.0187

TABLE 10 (Continued)

Run No.	G_l #/Hr-Ft^2	G_{Air} #/Hr-Ft^2	ϕ_w	f_w
339	66,100	9,150	.108	.0165
340	66,600	10,950	.0796	.0171
331	67,400	12,350	.0660	.0178
341	66,600	13,600	.0541	.0209
332	66,600	15,400	.0445	.0233
342	66,600	18,200	.0327	.0281
333	66,600	20,800	.0262	.0331
343	66,600	24,000	.0207	.0401
353	89,200	3,820	.923	.00932
354	89,200	5,400	.490	.00868
355	90,000	7,100	.302	.00803
356	90,000	9,050	.196	.00790
357	90,000	11,450	.129	.00855
359	90,000	12,500	.110	.00901
358	90,000	13,850	.0927	.00964
360	90,000	15,600	.0752	.0103
361	90,000	18,000	.0582	.0115

CHAPTER V

DISCUSSION OF RESULTS

Flow Pattern Description

Nomenclature for the various flow types encountered is shown in Figure 3. The general description of each is as follows:

Ripple; The fluids flow in two layers with small rounded ripples at the interface.

Wave; The fluids flow in two layers as in ripple flow, but due to a higher air velocity the interface contains irregular, sharp-peaked waves.

Slug; An occasional frothy mass of liquid is picked up by the air, and as the liquid fills the complete cross section of the pipe it is accelerated by the gas to a higher velocity than the average liquid velocity. Air behind the slug is compressed causing pressure fluctuations.

Crest; Similar to slug flow, but the liquid picked up by the air fails to fill the complete pipe cross section and is therefore not accelerated. Pressure fluctuations are not as severe.

Semi-annular; A rough, wavy, moving liquid film covers the entire pipe wall. The liquid layer is thickest on the bottom section of the pipe. Air moves at a high velocity through the central core of the pipe.

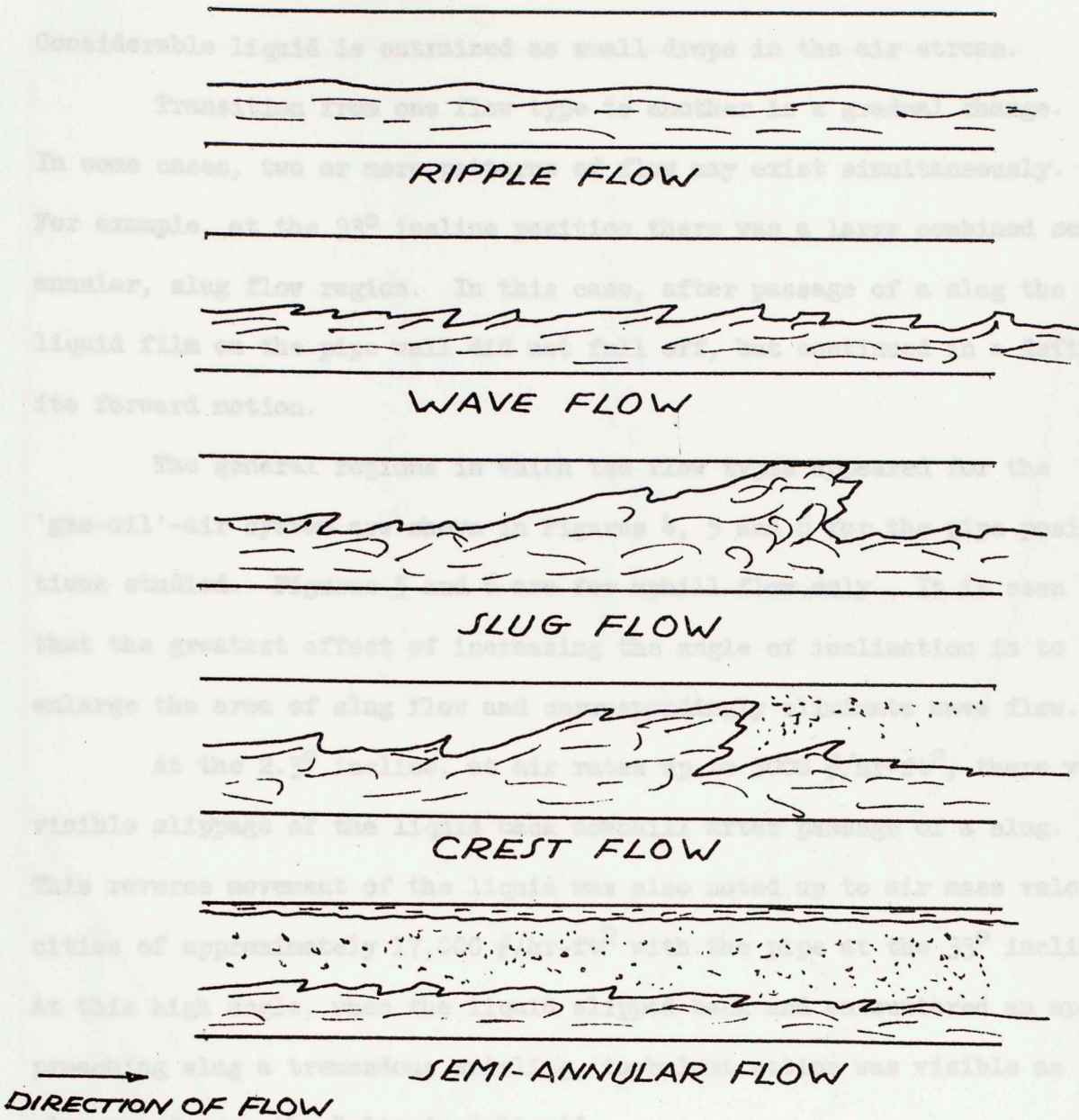

FIGURE 3. SKETCH OF FLOW PATTERNS

Considerable liquid is entrained as small drops in the air stream.

Transition from one flow type to another is a gradual change. In some cases, two or more patterns of flow may exist simultaneously. For example, at the 33° incline position there was a large combined semi-annular, slug flow region. In this case, after passage of a slug the liquid film on the pipe wall did not fall off, but continued in a definite forward motion.

The general regions in which the flow types appeared for the 'gas-oil'-air system are shown in Figures 4, 5 and 6 for the pipe positions studied. Figures 5 and 6 are for uphill flow only. It is seen that the greatest effect of increasing the angle of inclination is to enlarge the area of slug flow and correspondingly eliminate wave flow.

At the 2.3° incline, at air rates up to 5000 #/hr-ft^2, there was visible slippage of the liquid back downhill after passage of a slug. This reverse movement of the liquid was also noted up to air mass velocities of approximately 17,000 #/hr-ft^2 with the pipe at the 33° incline. At this high angle, when the liquid slipped back and encountered an approaching slug a tremendous swirling, turbulent action was visible as the slug moved over the "slipping" liquid.

Raising the test section to a steeper slope increased the number of slugs per unit time. Slug frequencies up to 15 per minute appeared in horizontal flow. At 2.3° the number per minute ranged from 10, at low liquid mass velocities, to 25 at the highest liquid mass velocity. At the 33° angle there was a frequency range of 40 to 60 slugs per minute at all liquid rates.

Comparison of the 'gas-oil'-air and water-air systems shows that,

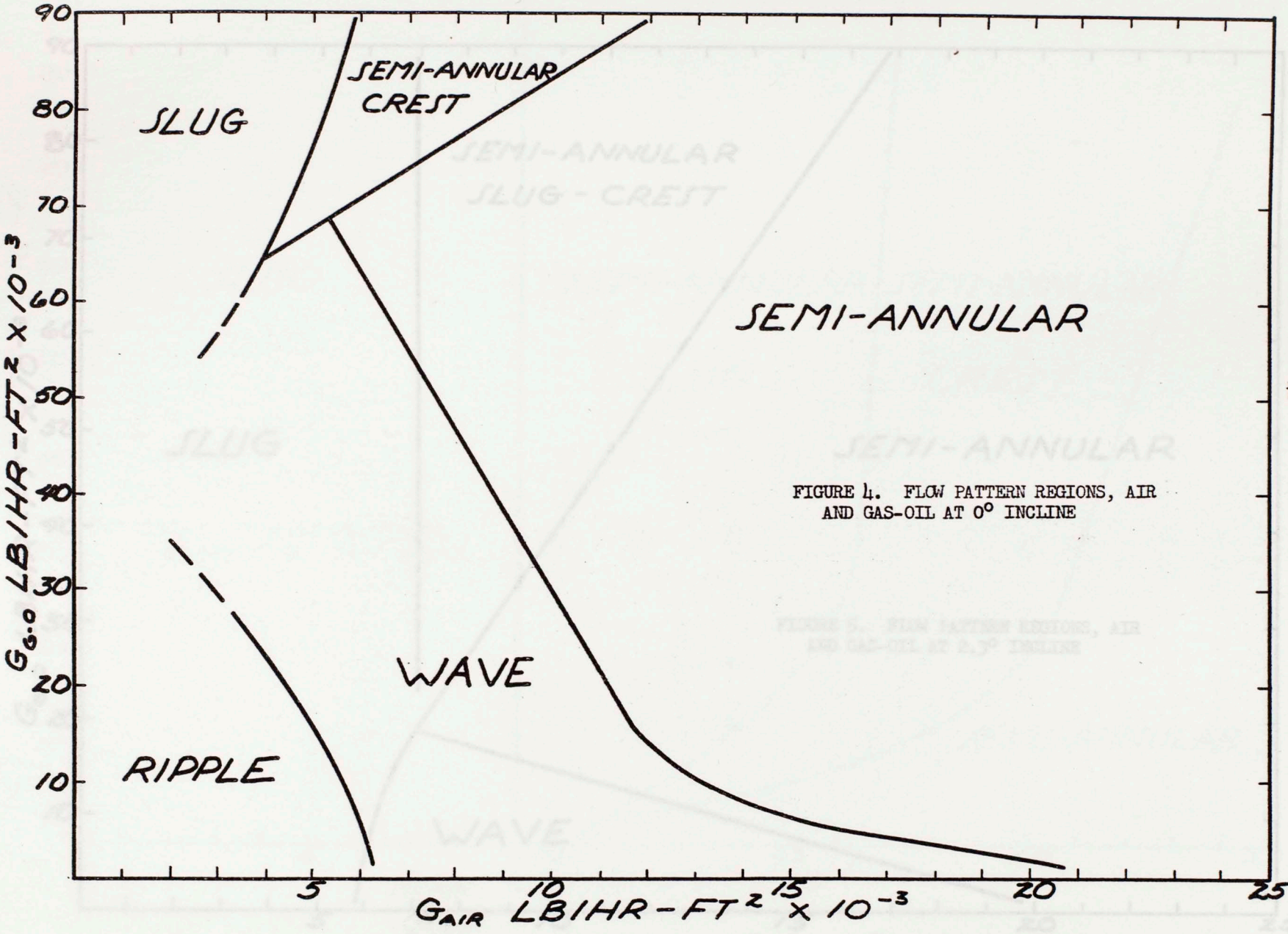

FIGURE 4. FLOW PATTERN REGIONS, AIR AND GAS-OIL AT 0° INCLINE

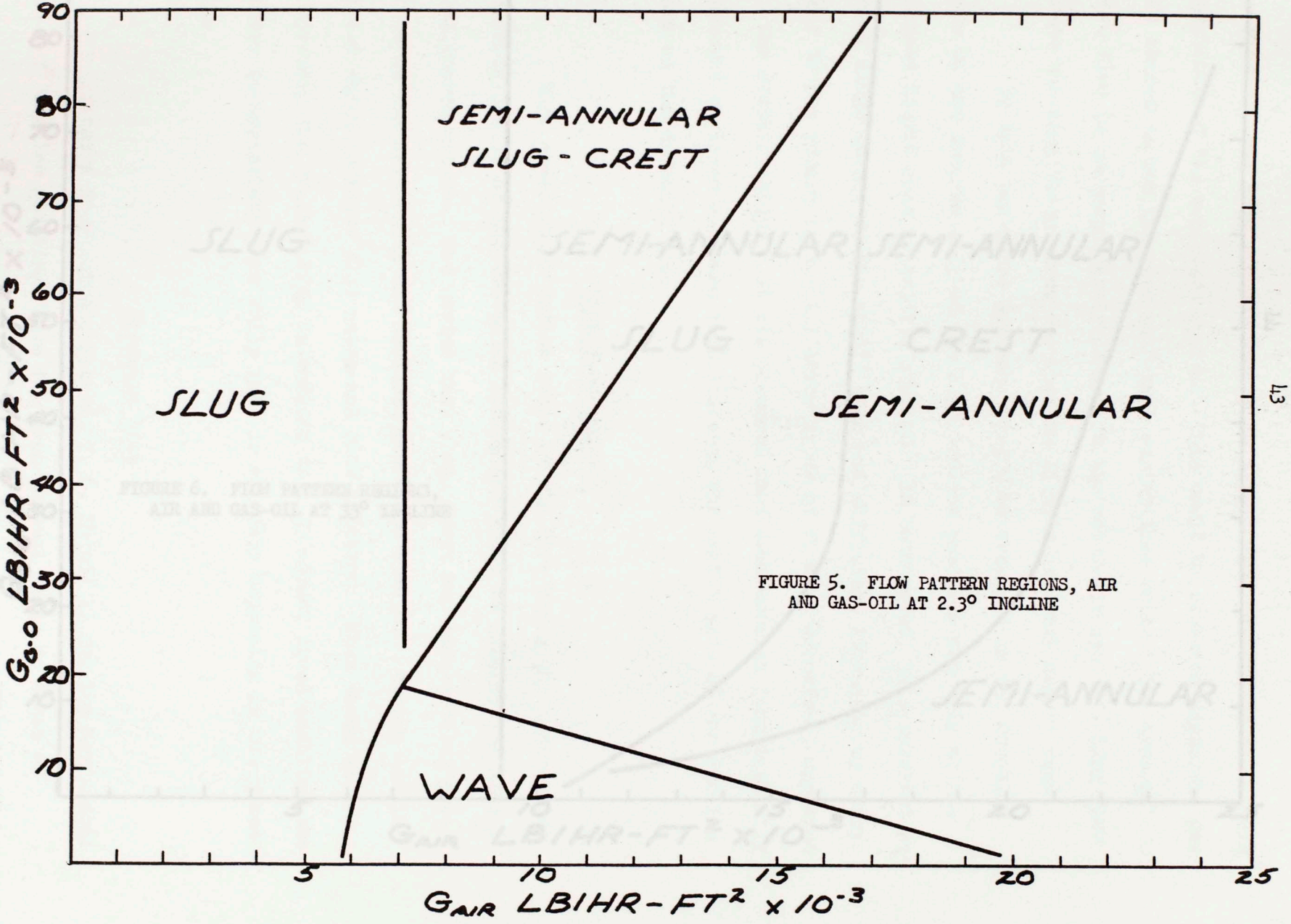

FIGURE 5. FLOW PATTERN REGIONS, AIR AND GAS-OIL AT 2.3° INCLINE

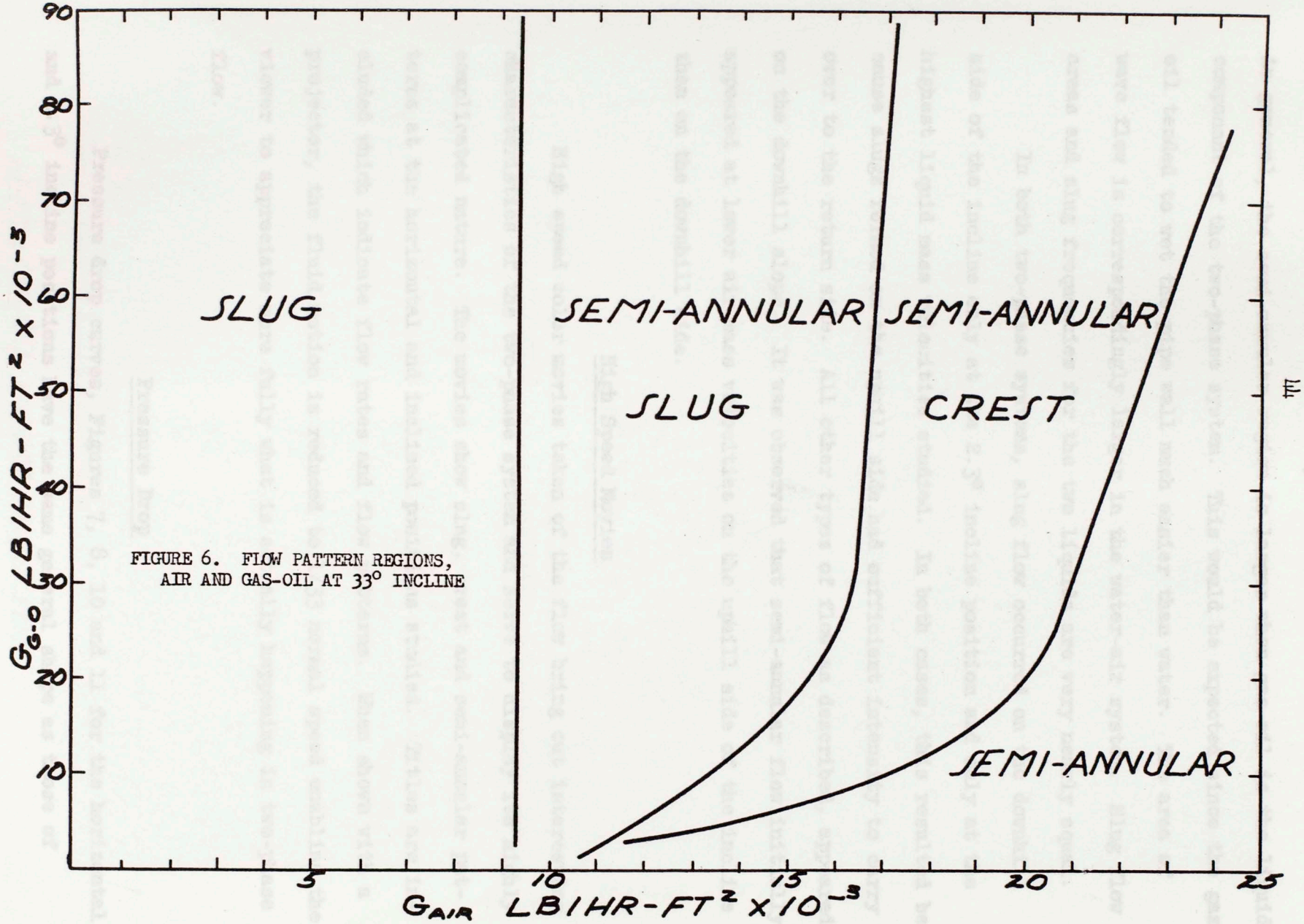

FIGURE 6. FLOW PATTERN REGIONS, AIR AND GAS-OIL AT 33° INCLINE

in general, the semi-annular region is larger when gas-oil is the liquid component of the two-phase system. This would be expected since the gas-oil tended to wet the pipe wall much easier than water. The area of wave flow is correspondingly larger in the water-air system. Slug flow areas and slug frequencies for the two liquids are very nearly equal.

In both two-phase systems, slug flow occurred on the downhill side of the incline only at the 2.3° incline position and only at the highest liquid mass velocities studied. In both cases, this resulted because slugs formed on the uphill side had sufficient intensity to carry over to the return side. All other types of flow as described, appeared on the downhill slope. It was observed that semi-annular flow initially appeared at lower air mass velocities on the uphill side of the incline than on the downhill side.

High Speed Movies

High speed color movies taken of the flow bring out interesting characteristics of the two-phase system and serve to display its highly complicated nature. The movies show slug, crest and semi-annular patterns at the horizontal and inclined positions studied. Titles are included which indicate flow rates and flow patterns. When shown with a projector, the fluid motion is reduced to 1/33 normal speed enabling the viewer to appreciate more fully what is actually happening in two-phase flow.

Pressure Drop

Pressure drop curves, Figures 7, 8, 10 and 11 for the horizontal and 2.3° incline positions have the same general shape as those of

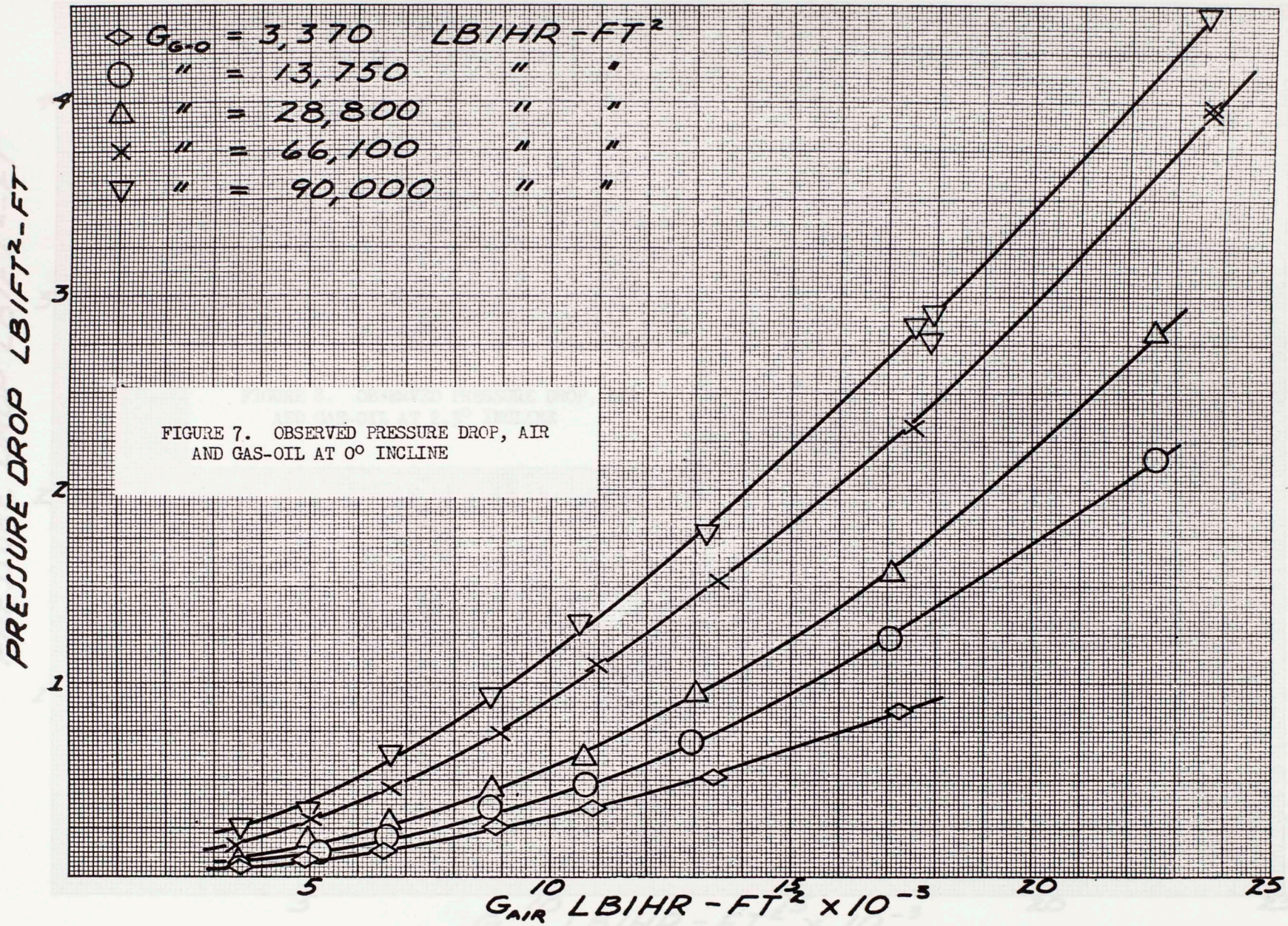

FIGURE 7. OBSERVED PRESSURE DROP, AIR AND GAS-OIL AT 0° INCLINE

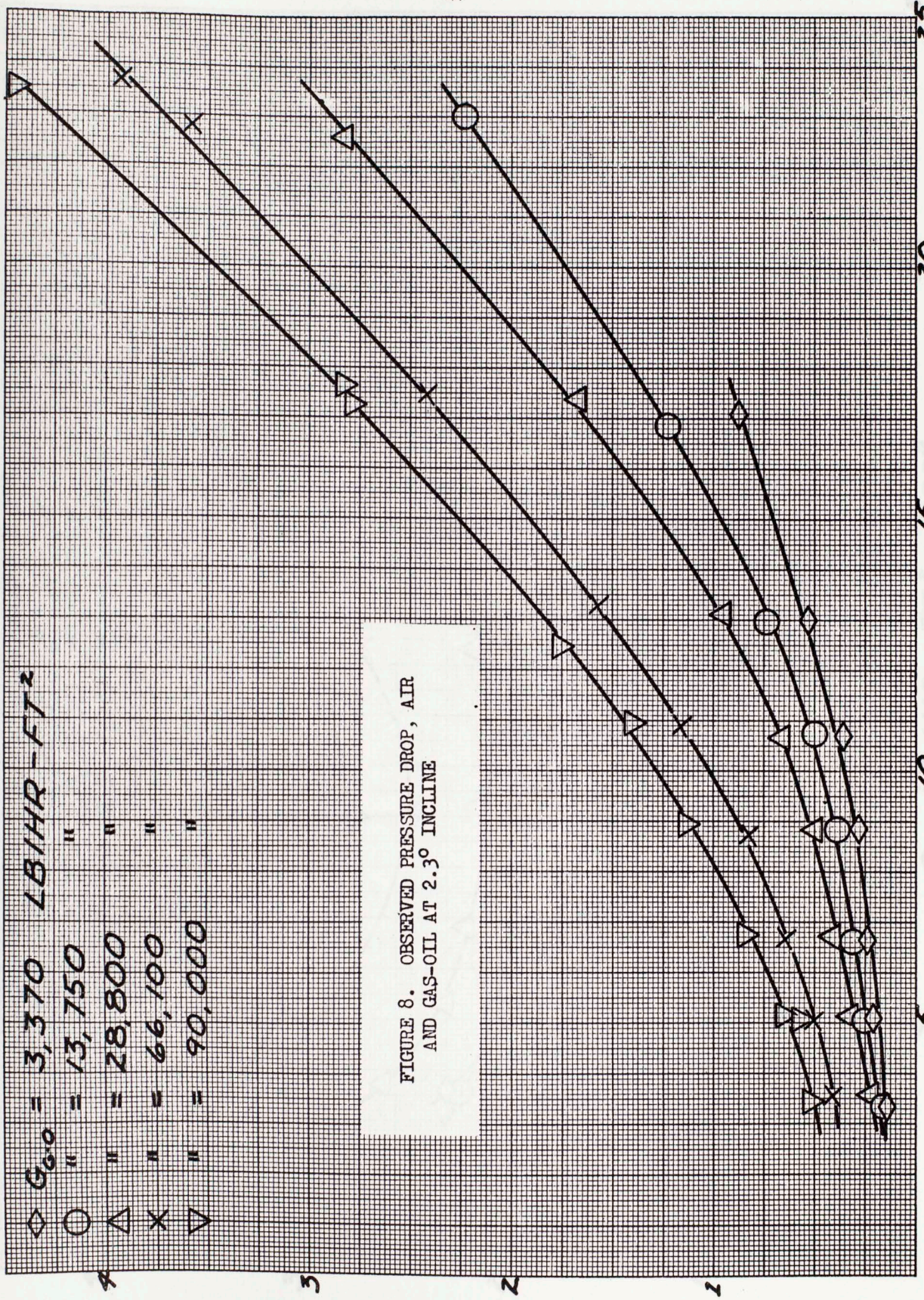

FIGURE 8. OBSERVED PRESSURE DROP, AIR AND GAS-OIL AT 2.3° INCLINE

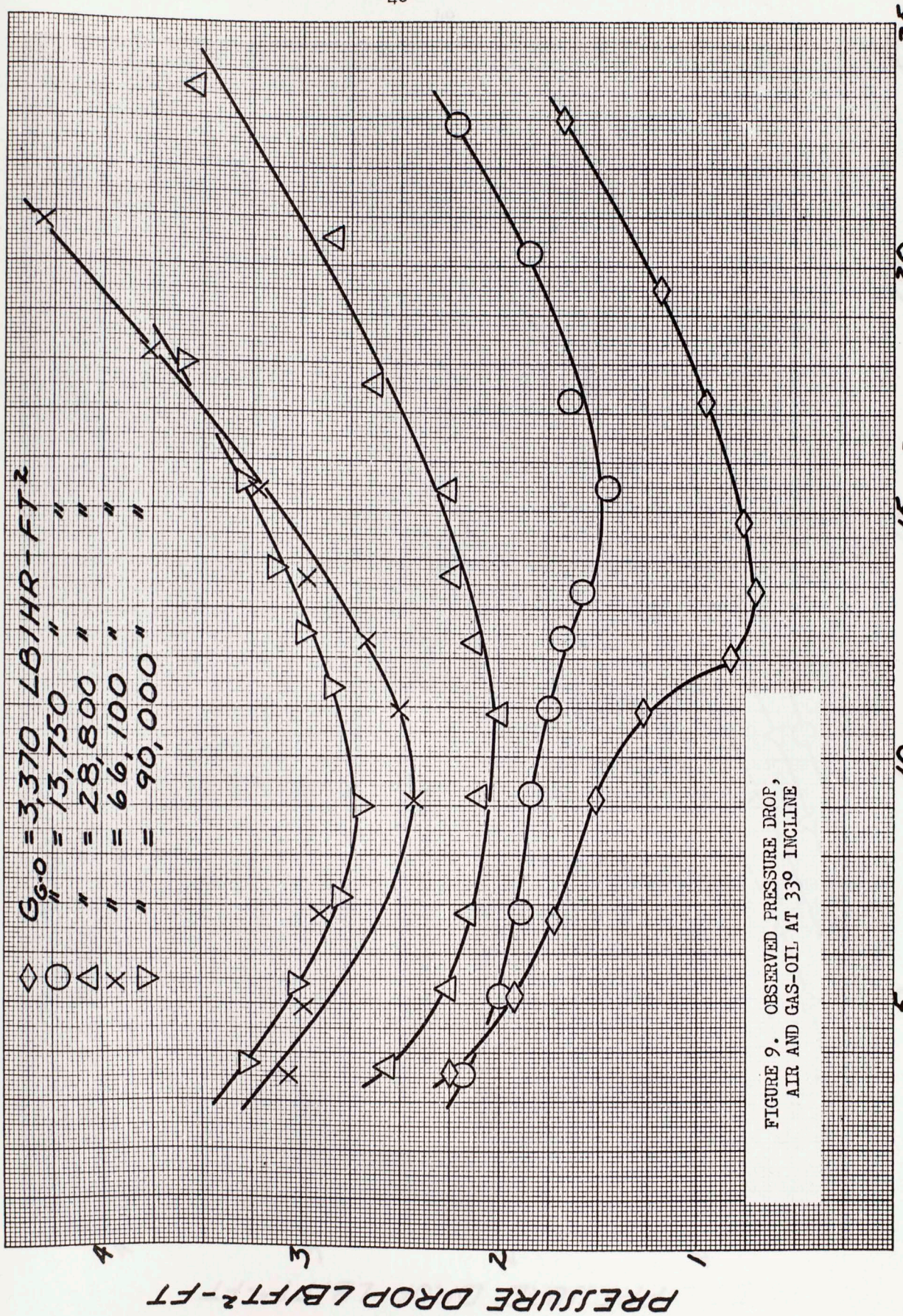

FIGURE 9. OBSERVED PRESSURE DROP, AIR AND GAS-OIL AT 33° INCLINE

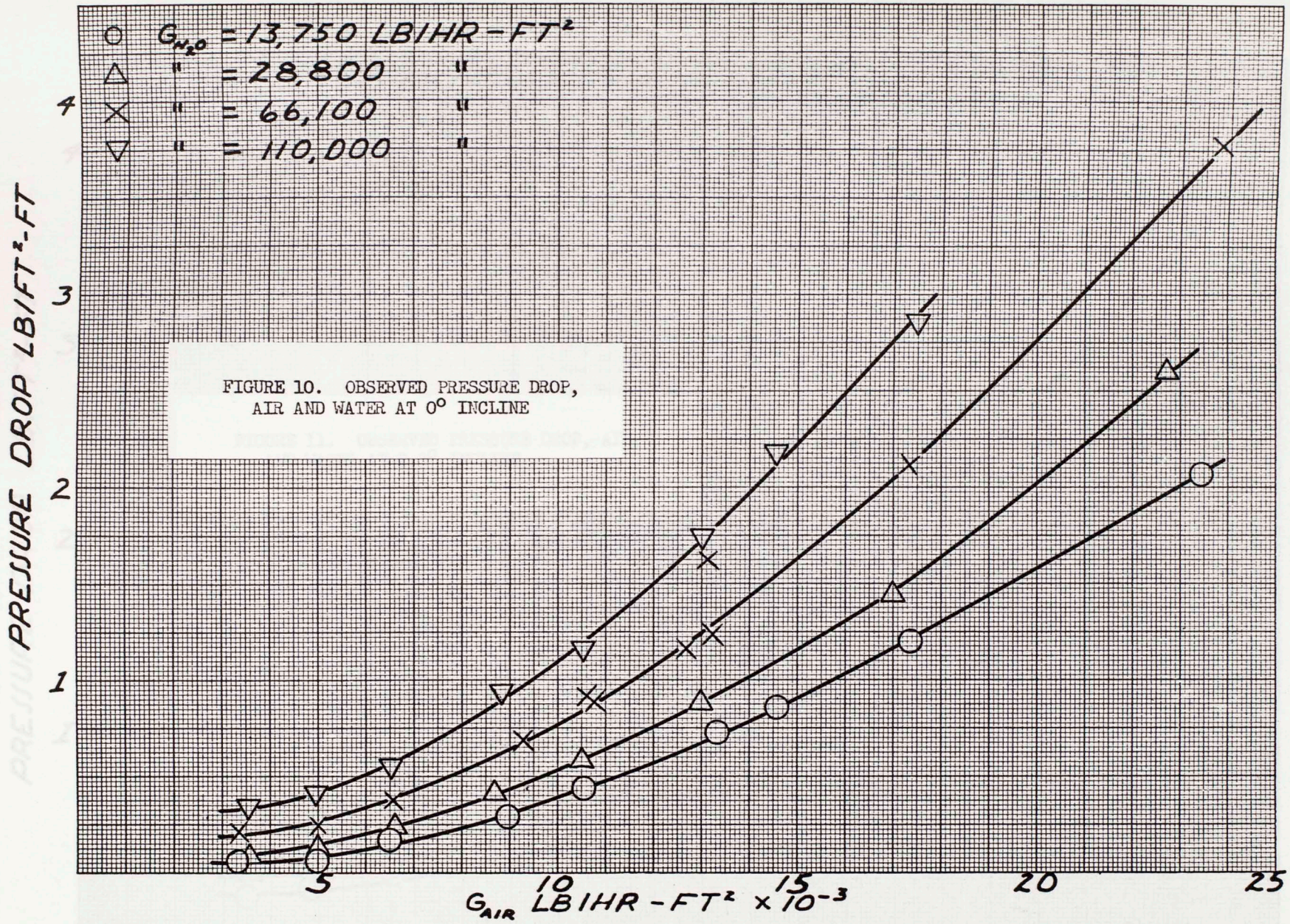

FIGURE 10. OBSERVED PRESSURE DROP, AIR AND WATER AT 0° INCLINE

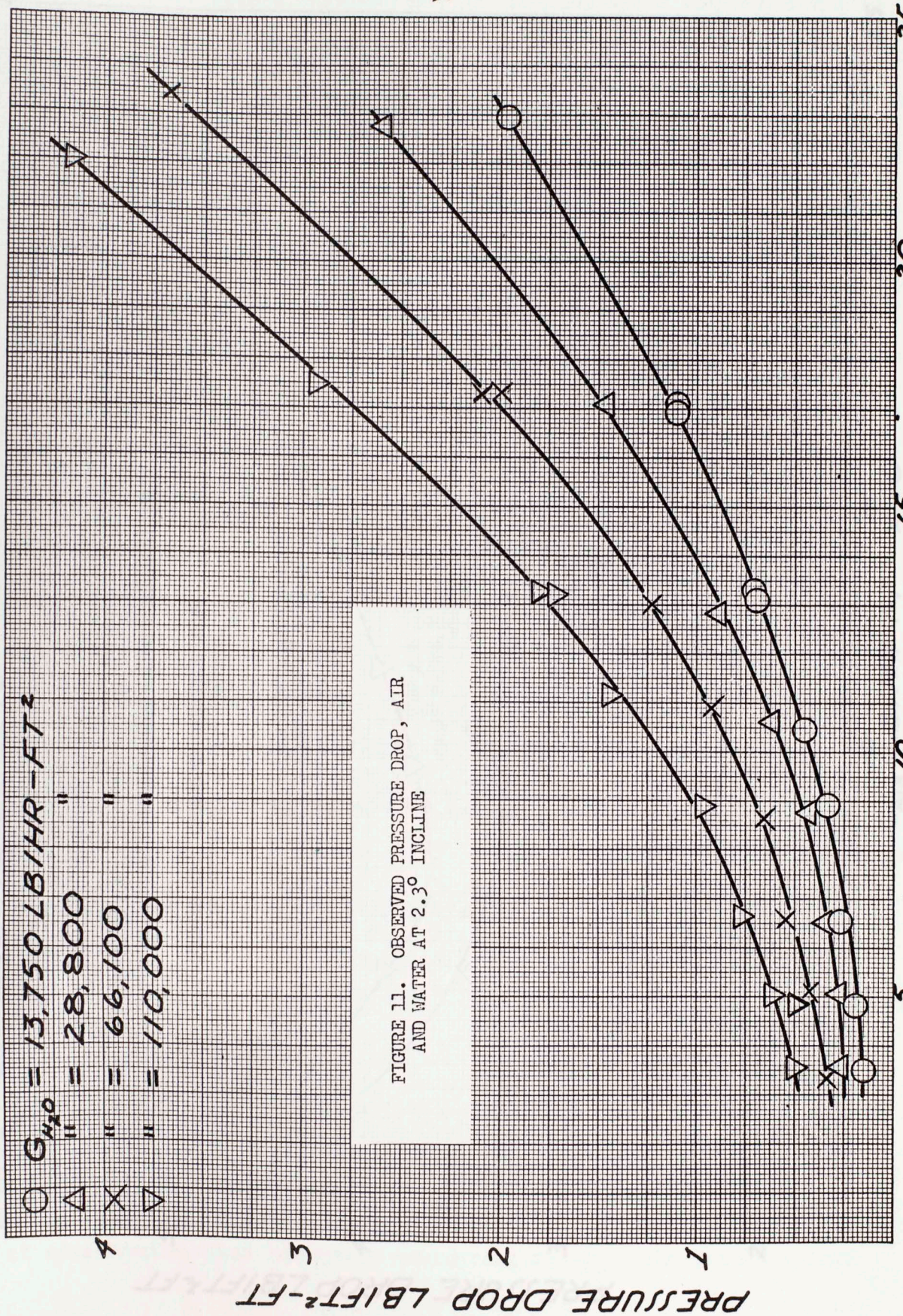

FIGURE 11. OBSERVED PRESSURE DROP, AIR AND WATER AT 2.3° INCLINE

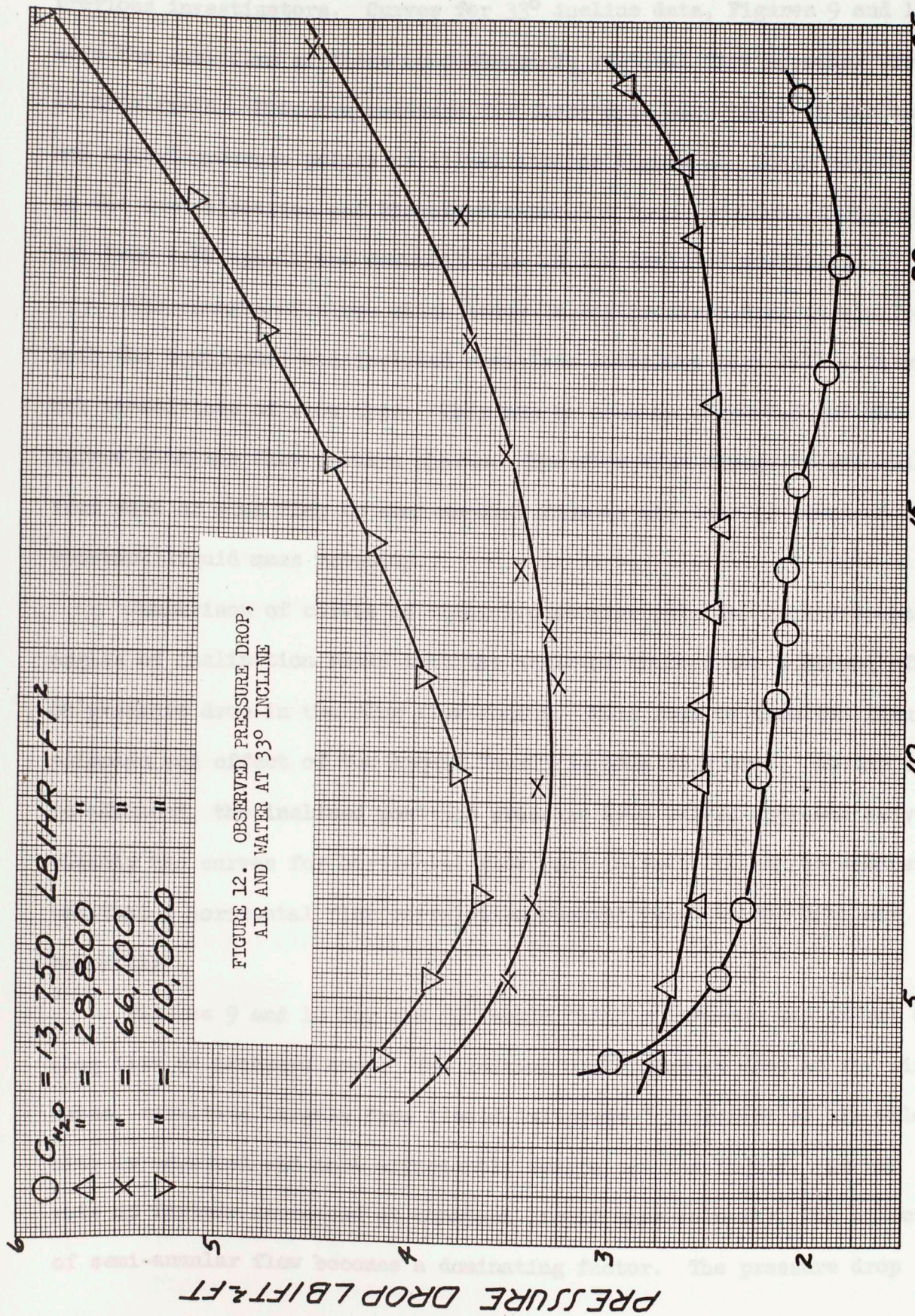

FIGURE 12. OBSERVED PRESSURE DROP, AIR AND WATER AT 33° INCLINE

previous investigators. Curves for 33° incline data, Figures 9 and 12 have the same form as those encountered in vertical flow by other workers in this field. Pressure readings for these data were taken at the inlet and outlet pressure points as illustrated in Figure 1. These points were at the same elevation and therefore represent total pressure drop resulting from both uphill and downhill flow in the inclined positions.

The changes of slope which occur in the pressure drop curves for both the horizontal and inclined positions correlate very well with visual transitions of flow type. This may be seen by comparison of the curves with the flow pattern charts. The flow type change is generally from wave or slug flow to semi-annular flow as air rate is advanced at constant liquid mass velocity.

Comparison of curves of equal liquid flow rate but at different angles of inclination shows that the angle of incline has a strong effect on pressure drop in the slug flow region. This results from the liquid slippage and effect of the liquid "head" in this flow area. As air rate is advanced, the inclined position pressure drop curves approach very closely the curves for horizontal flow, and in fact, it can be demonstrated that a horizontal flow correlation becomes valid at the high air velocities.

Figures 9 and 12 for the 33° angle clearly indicate the effect of slug flow on pressure drop. The initial high pressure drop at low air rates, resulting largely from liquid "slippage," decreases as air velocity is advanced and more efficiently sweeps out the liquid. As air rate is further increased at constant liquid mass velocity, the effect of semi-annular flow becomes a dominating factor. The pressure drop

curve passes through a minimum and begins to increase with the higher air flow. The inflection points in curves of low liquid mass velocities in Figures 9 and 12 result from a rapid change of flow type from slug to semi-annular which occurred in these regions.

From the pressure drop curves of the 'gas-oil'-air and water-air systems, it is seen that for the horizontal and 2.3° inclines at a given liquid mass velocity, the pressure drop is generally higher in the 'gas-oil'-air system. This is a result mainly of two factors: (1) the higher viscosity of gas-oil, and (2) the tendency of gas-oil to wet the pipe wall initiating semi-annular flow at lower air rates than with water.

At the 33° incline, at a specified liquid mass velocity, and at the lower air rates, the pressure drop is larger in the water-air system than in the 'gas-oil'-air system. The higher density of water is the controlling factor at these low air rates as a result of liquid slippage. However, at the higher air rates studied (above 17,000 #/hr-ft^2), the 'gas-oil'-air system pressure drop again becomes greater as in horizontal and low angle flow.

White Correlation

A correlation of horizontal 'gas-oil'-air pressure drop data with the development of White[24] is shown in Figure 13. The maximum deviation is plus or minus 30 per cent neglecting ripple and slug type flow. A similar plot for the water-air system gives maximum deviations of plus or minus 35 per cent. In both cases the average deviation is much less. Equations for the White functions with coordinates for Figure 13 are listed in Table 9.

Figure 14 is a comparison of the 'gas-oil'-air data taken at a

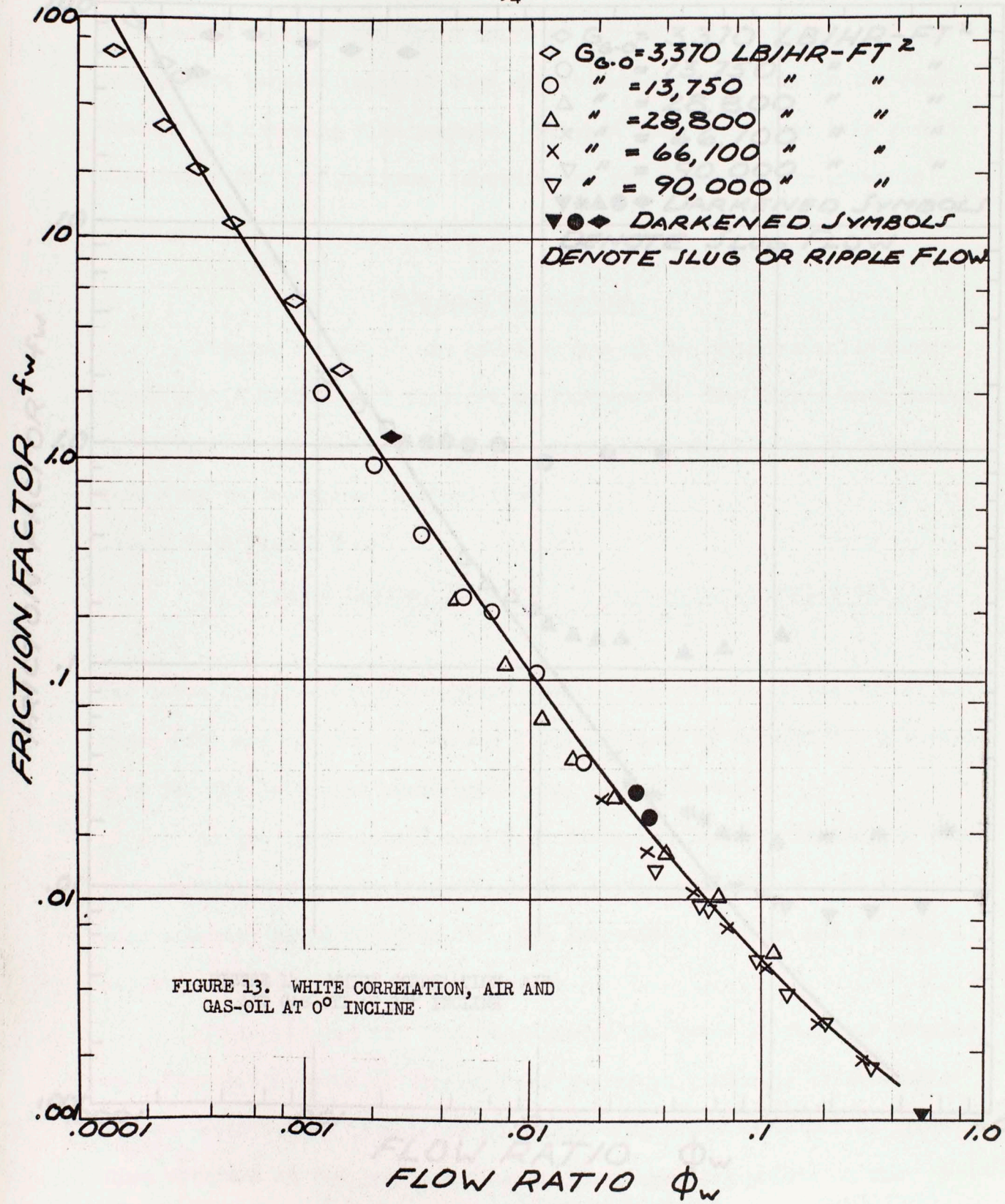

FIGURE 13. WHITE CORRELATION, AIR AND GAS-OIL AT 0° INCLINE

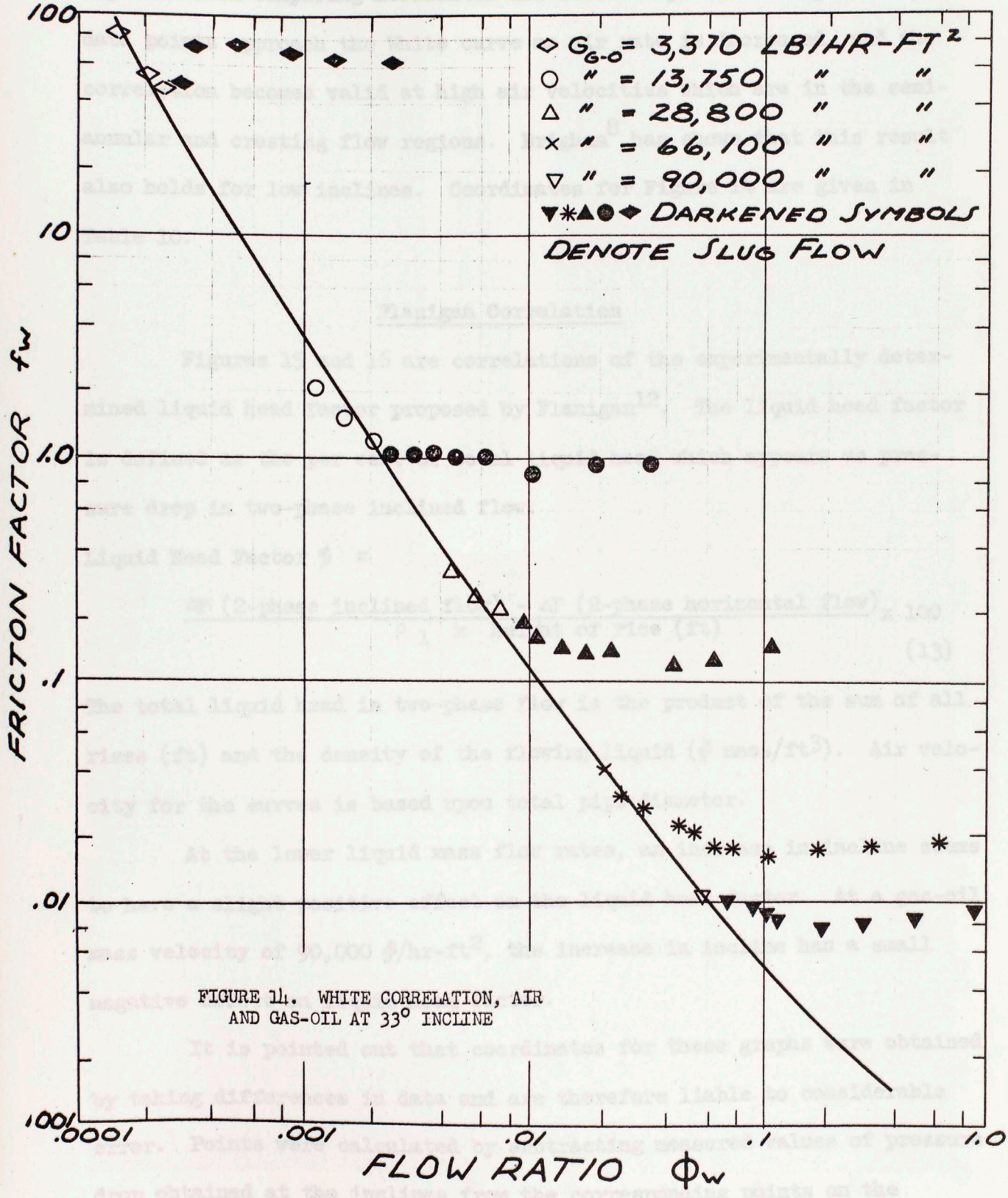

FIGURE 14. WHITE CORRELATION, AIR AND GAS-OIL AT 33° INCLINE

33° incline with the White correlation for horizontal flow. As would be expected from comparing horizontal and inclined pressure drop curves, the data points approach the White curve as air rate is increased, and the correlation becomes valid at high air velocities which are in the semi-annular and cresting flow regions. Brigham[8] has shown that this result also holds for low inclines. Coordinates for Figure 14 are given in Table 10.

Flanigan Correlation

Figures 15 and 16 are correlations of the experimentally determined liquid head factor proposed by Flanigan[12]. The liquid head factor is defined as the per cent of total liquid head which appears as pressure drop in two-phase inclined flow.

Liquid Head Factor % =

$$\frac{\Delta P \text{ (2-phase inclined flow)} - \Delta P \text{ (2-phase horizontal flow)}}{\rho_1 \times \text{height of rise (ft)}} \times 100 \qquad (13)$$

The total liquid head in two-phase flow is the product of the sum of all rises (ft) and the density of the flowing liquid (# mass/ft^3). Air velocity for the curves is based upon total pipe diameter.

At the lower liquid mass flow rates, an increase in incline seems to have a slight positive effect on the liquid head factor. At a gas-oil mass velocity of 90,000 #/hr-ft^2, the increase in incline has a small negative effect on liquid head factor.

It is pointed out that coordinates for these graphs were obtained by taking differences in data and are therefore liable to considerable error. Points were calculated by subtracting measured values of pressure drop obtained at the inclines from the corresponding points on the

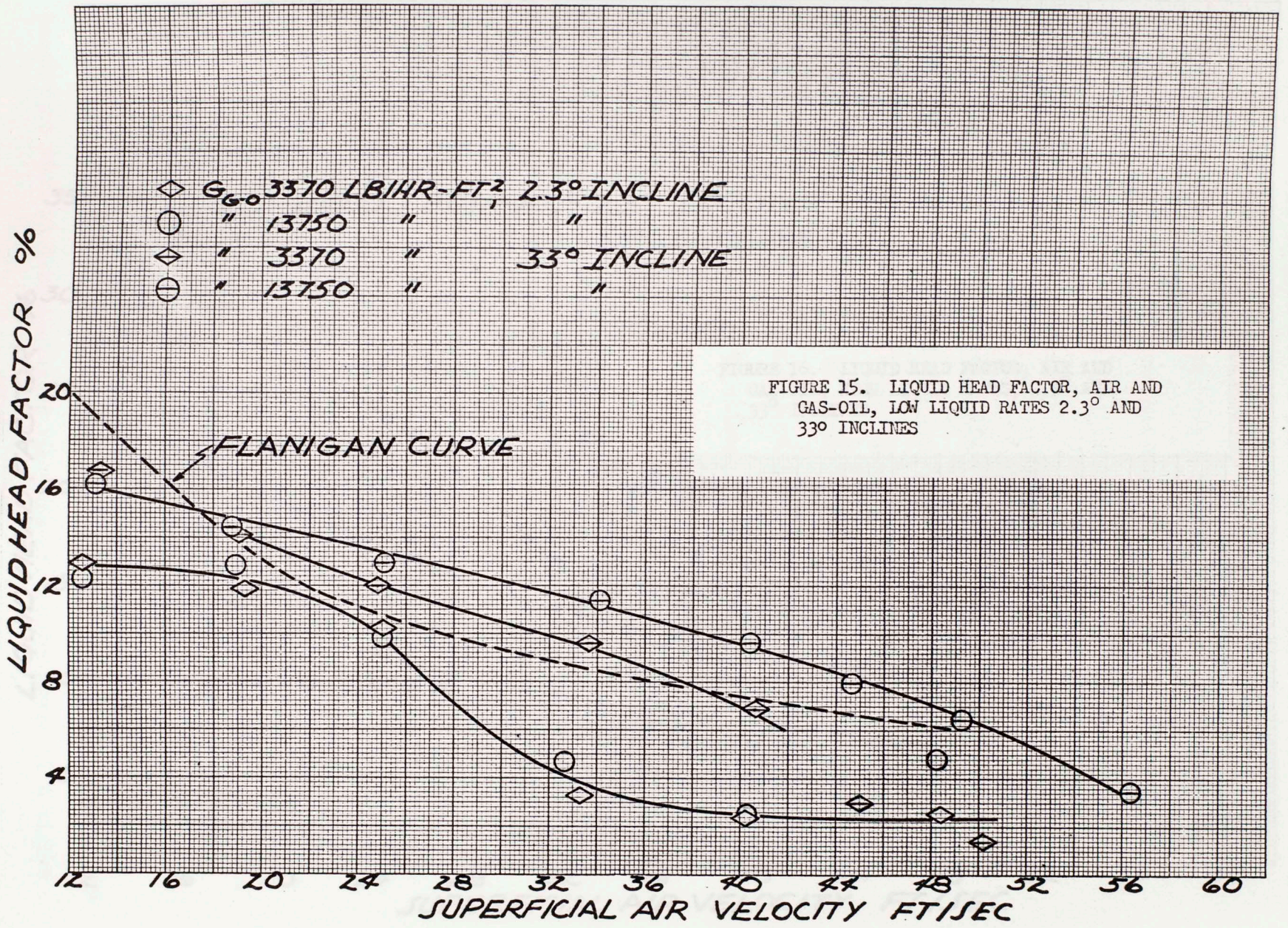

FIGURE 15. LIQUID HEAD FACTOR, AIR AND GAS-OIL, LOW LIQUID RATES 2.3° AND 33° INCLINES

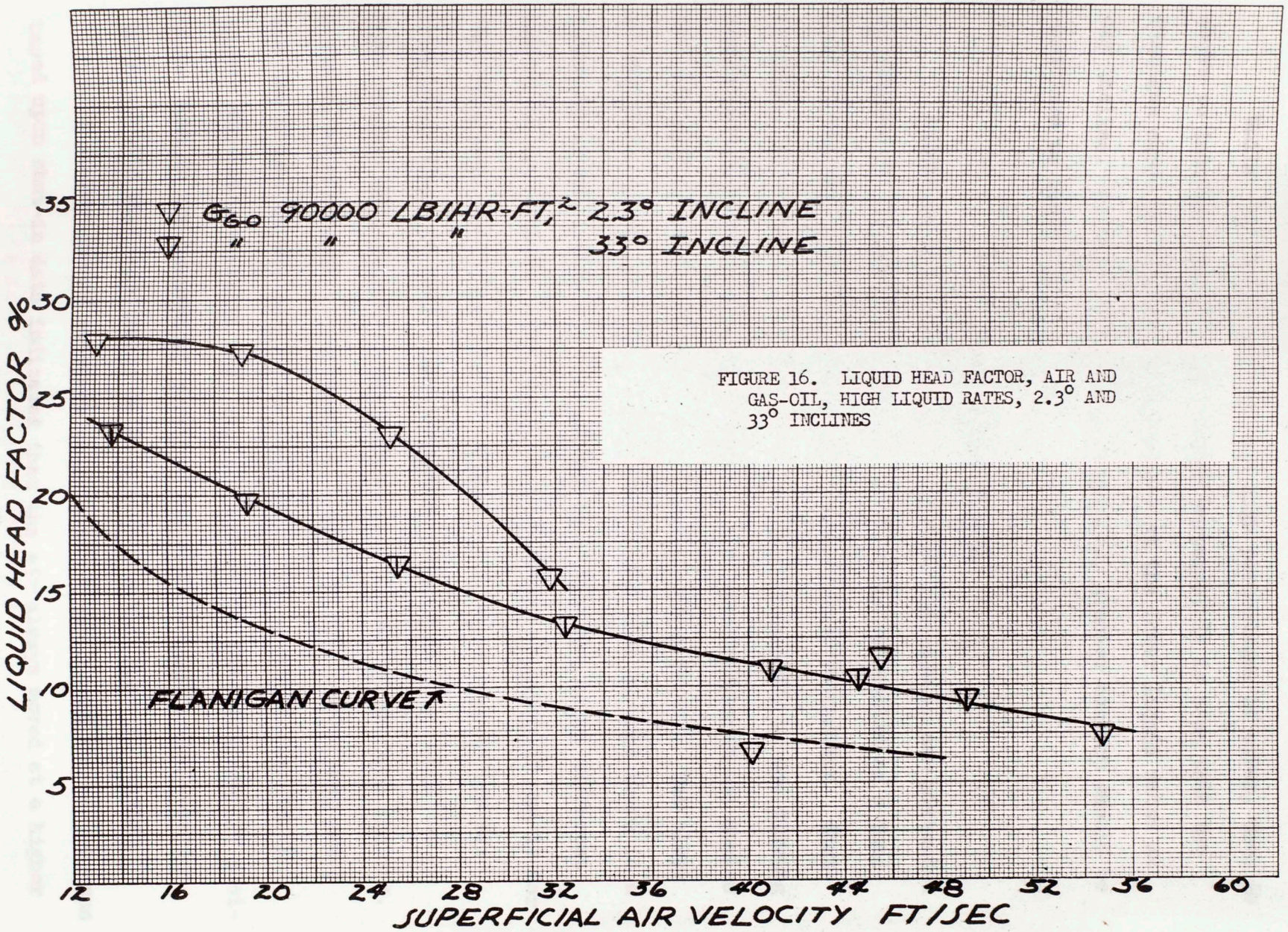

FIGURE 16. LIQUID HEAD FACTOR, AIR AND GAS-OIL, HIGH LIQUID RATES, 2.3° AND 33° INCLINES

horizontal two-phase pressure drop curve.

While the curves may exhibit high percentages of error, they do serve to indicate a trend. For design purposes, it is seen that the Flanigan curve is a fairly good estimate at the lower liquid rates at any incline. At high liquid mass velocities, greater caution should be exercised as would be expected.

Liquid In-Place Data

Liquid in-place data for the 'gas-oil'-air system are presented in Figures 17, 18 and 19 where the shut-in ratio is plotted as a function of air mass velocity with liquid mass velocity parameters. Shut-in ratio is defined as ft^3 air in-place/ft^3 oil in-place at the flowing conditions of temperature and pressure. The relationship at all angles is very nearly linear above an air rate of 10,000 #/hr-ft^2. The slope of the curve varies inversely with the angle of incline, and there is a crossing of two curves of equal liquid mass velocity but at different angles of inclination. For example, comparison of Figures 17 and 19 for the horizontal and 33° positions respectively, shows that at low air velocities there is more liquid in-place in the horizontal position. This results from slug flow sweeping out the liquid at the high incline. However, as air input is increased it begins to more effectively sweep out the liquid in the horizontal position. The result is that at the higher air rates there is more liquid in-place in the inclined flow positions than in the horizontal position for a given liquid mass velocity. These results were also found to hold true for the water-air system.

A comparison of relative velocities of the liquid and air streams based upon shut-in data indicated that the air always moved at a higher

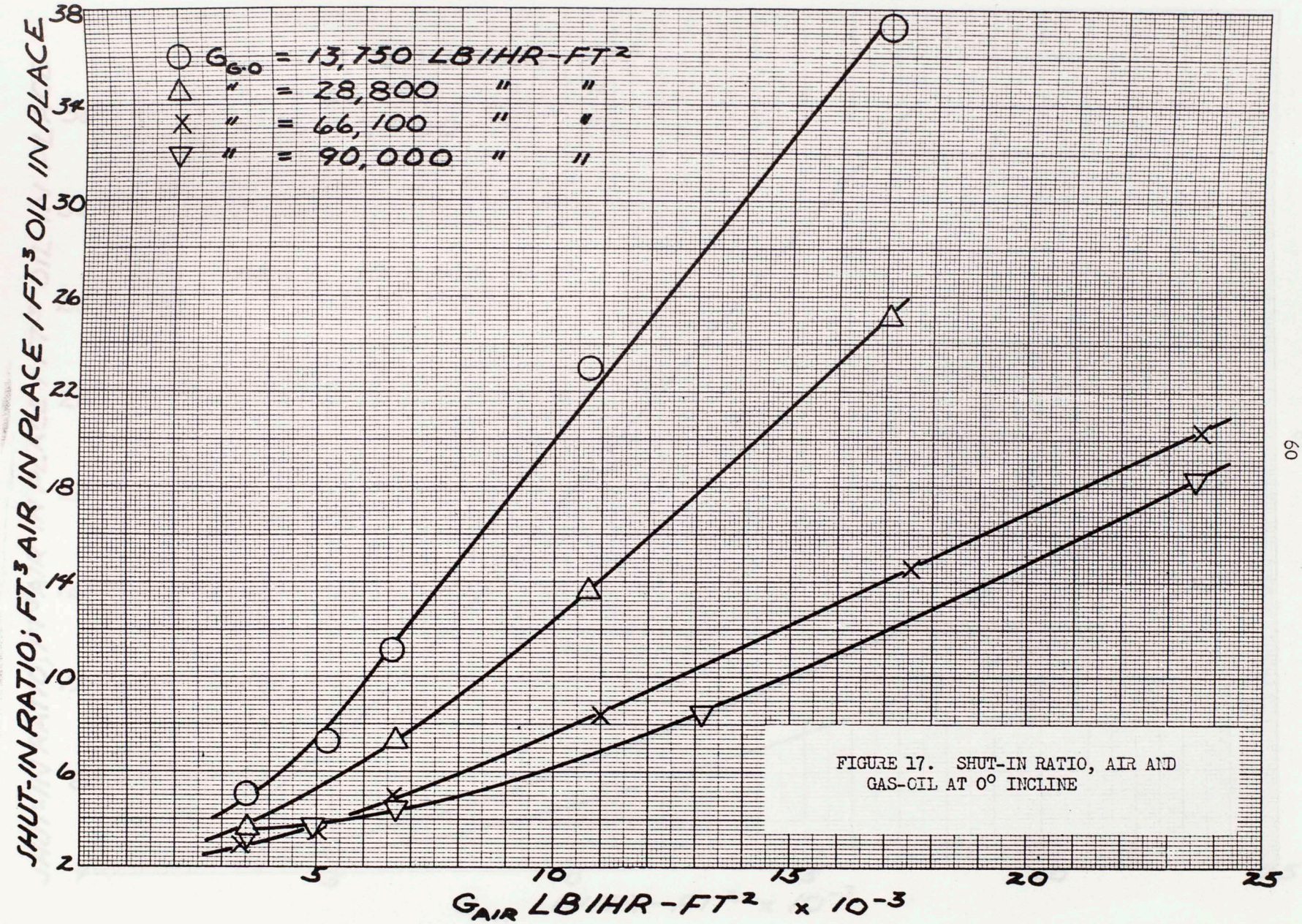

FIGURE 17. SHUT-IN RATIO, AIR AND GAS-OIL AT 0° INCLINE

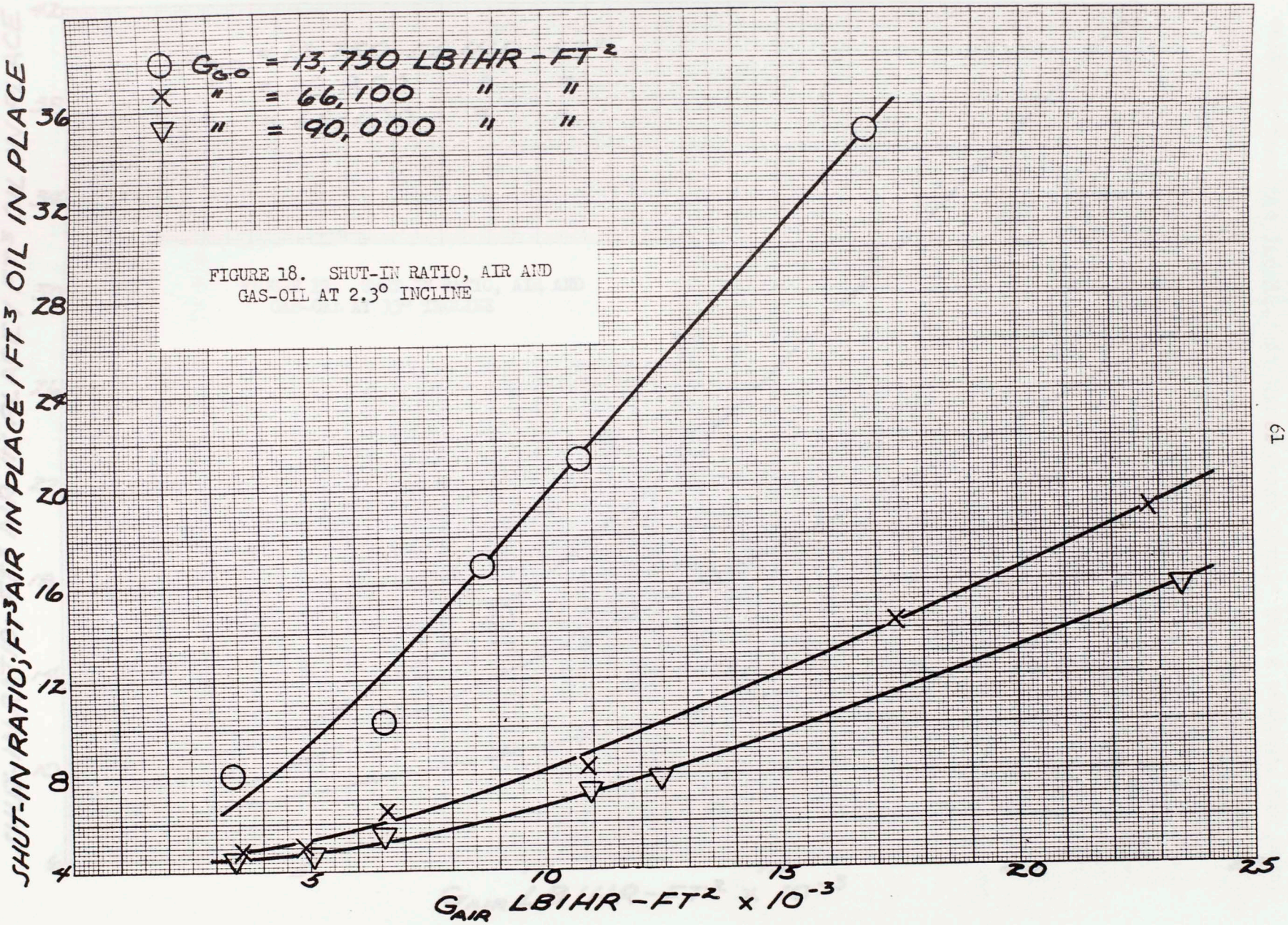

FIGURE 18. SHUT-IN RATIO, AIR AND GAS-OIL AT 2.3° INCLINE

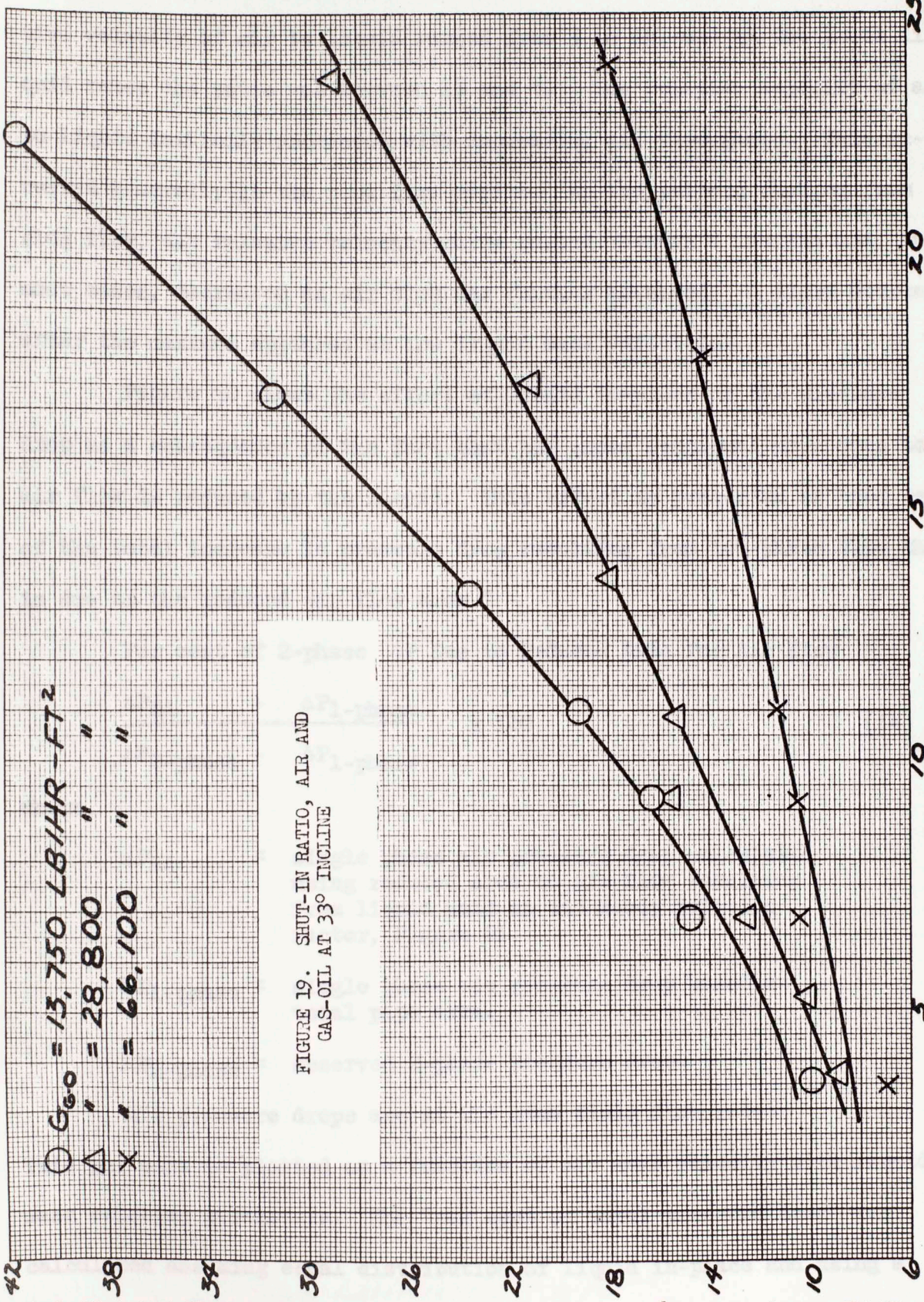

FIGURE 19. SHUT-IN RATIO, AIR AND GAS-OIL AT 33° INCLINE

velocity than the liquid. At the highest liquid rates studied, the relative velocity of air to liquid ranged from 5 to 16, and at the lower liquid rates the ratio was between 18 and 40. The relative velocity of air to liquid initially increased with increasing air throughout. This occurred generally in the slug flow region. As the pattern changed from slug flow, the relative velocity curve passed through a maximum and, in most cases, decreased as air flow was further advanced. A sharp decrease after the maximum appeared at low liquid mass velocities.

Figure 20 shows the effect of liquid in-place on the pressure drop as a consequence of the fact that the cross sectional area open to air flow is reduced by the liquid. This effect is presented as "per cent of the total increase in pressure drop resulting from two-phase flow that is due to the reduced air flow area."

Per cent of 2-phase ΔP Due to Reduced Area for Air Flow =

$$\frac{\Delta P_{RA} - \Delta P_{1\text{-phase}}}{\Delta P_{2\text{-phase}} - \Delta P_{1\text{-phase}}} \times 100 \qquad (14)$$

where,

ΔP_{RA} = single phase air pressure drop calculated using reduced area to air flow resulting from liquid hold-up and Moody friction factor, Figure 21.

$\Delta P_{1\text{-phase}}$ = single phase air pressure drop based on total pipe area.

$\Delta P_{2\text{-phase}}$ = observed 2-phase pressure drop.

All pressure drops are at the same fluid flow rates.

This per cent is plotted as a function of air mass velocity with liquid mass velocity parameters. The "per cent of total pressure drop" was calculated assuming equal distribution of liquid in-place and using a

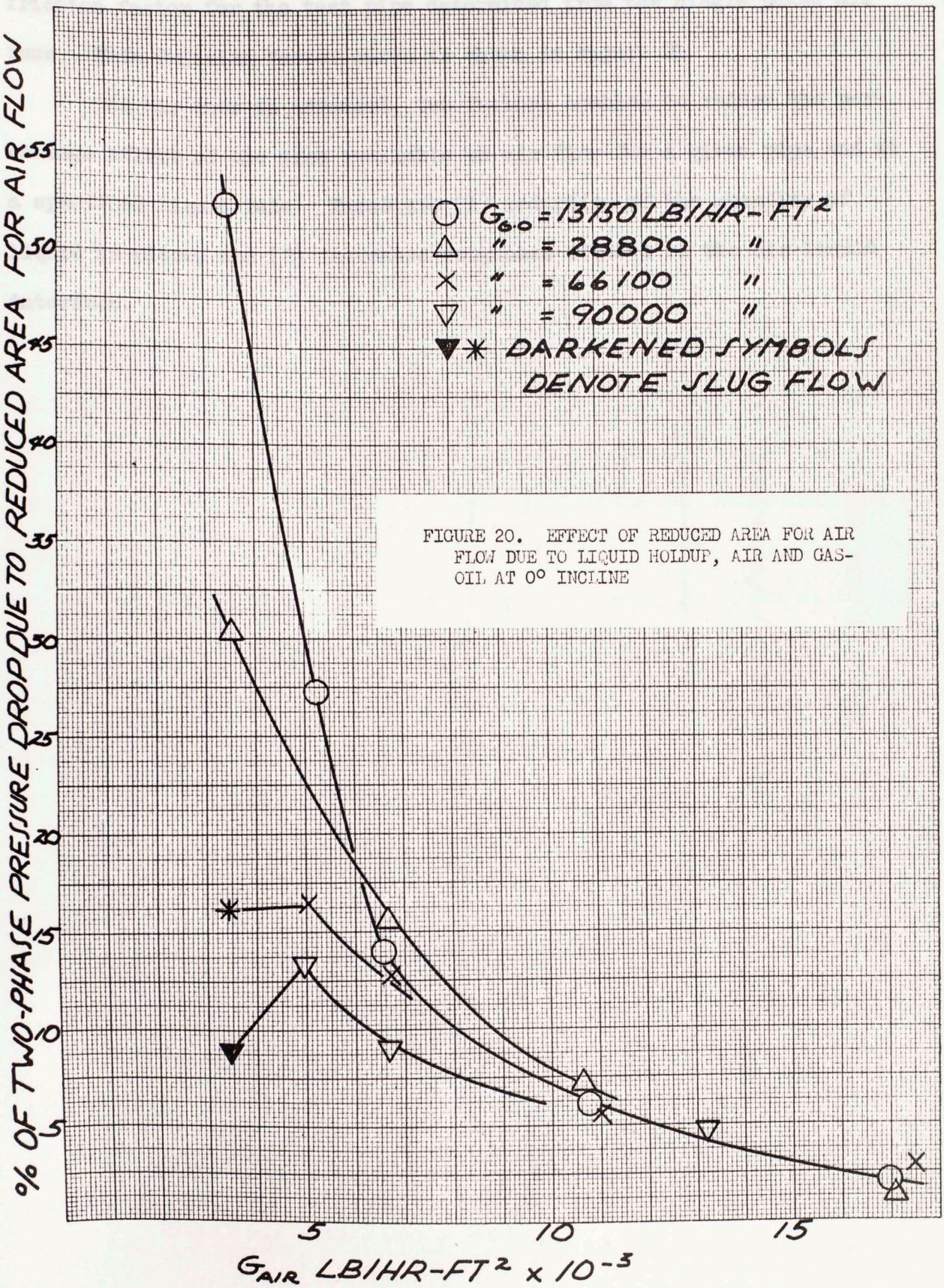

FIGURE 20. EFFECT OF REDUCED AREA FOR AIR FLOW DUE TO LIQUID HOLDUP, AIR AND GAS-OIL AT 0° INCLINE

friction factor for the test pipe determined from the single phase air runs. This friction factor curve is shown in Figure 21.

As air rate is advanced, two factors combine to reduce the percentage effect of the area available to air flow for a given pipe and at a specified liquid rate. These are (1) reduction of the quantity of liquid in-place, and (2) increased roughness effects of the air-liquid interface.

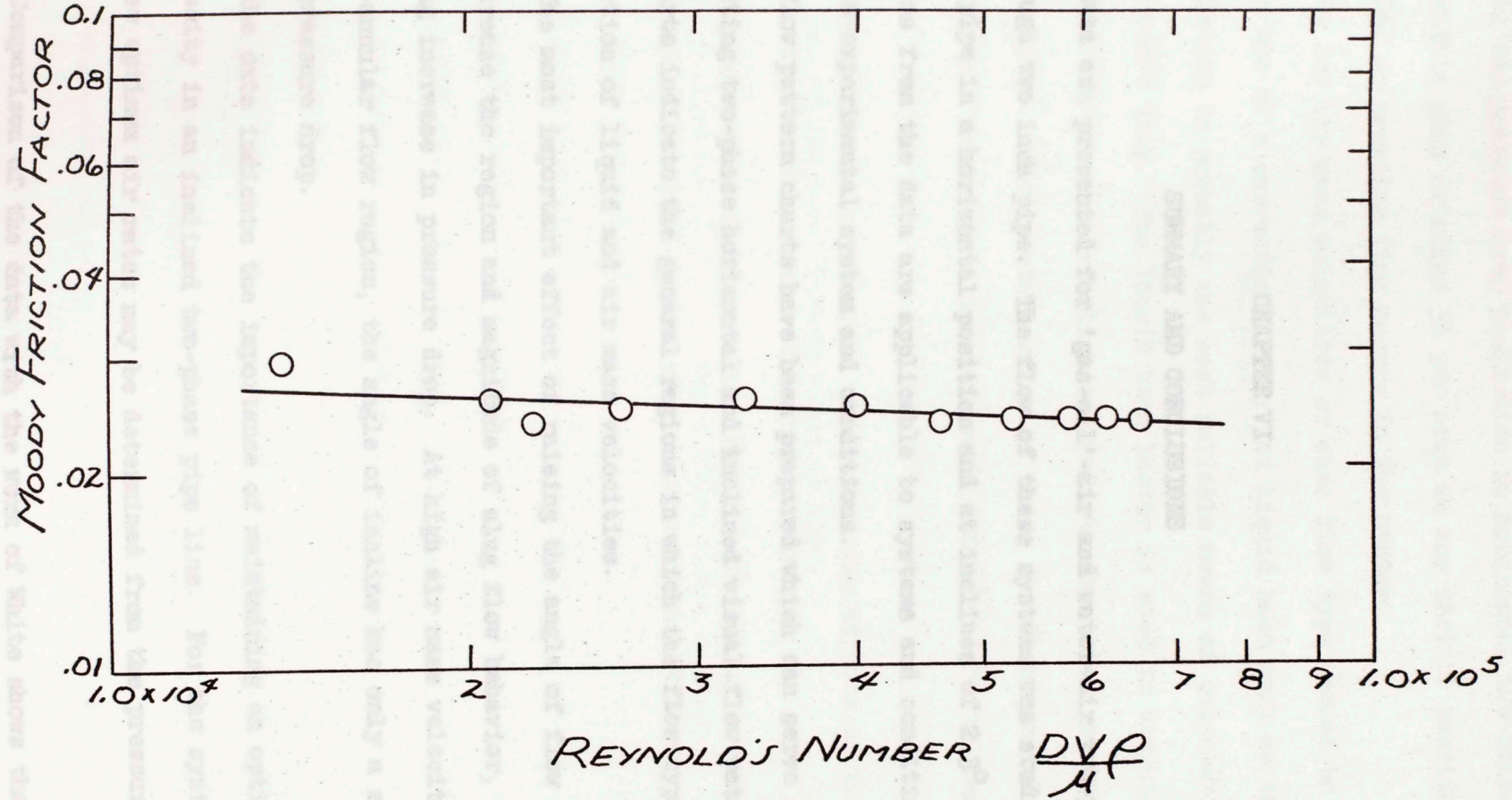

FIGURE 21. MOODY FRICTION FACTOR, SINGLE PHASE AIR FLOW

CHAPTER VI

SUMMARY AND CONCLUSIONS

Data are presented for 'gas-oil'-air and water-air two-phase flow through two inch pipe. The flow of these systems was studied with the test pipe in a horizontal position and at inclines of 2.3° and 33°. Conclusions from the data are applicable to systems and conditions similar to the experimental system and conditions.

Flow pattern charts have been prepared which can serve as a guide in predicting two-phase horizontal and inclined visual flow patterns. These charts indicate the general regions in which the flow types occur as a function of liquid and air mass velocities.

The most important effect of raising the angle of flow incline is to increase the region and magnitude of slug flow behavior, with corresponding increase in pressure drop. At high air mass velocities, in the semi-annular flow region, the angle of incline has only a small effect on pressure drop.

The data indicate the importance of maintaining an optimum gas mass velocity in an inclined two-phase pipe line. For the systems studied, these optimum air rates may be determined from the pressure drop curves.

Comparison of the data with the work of White shows that his

development for pressure drop prediction in horizontal two-phase flow is accurate within plus or minus 35 per cent at any incline position when semi-annular or cresting flow occurs in the system.

For low air mass velocities or when flow type cannot be determined, the use of a correction factor for liquid head such as the Flanigan correlation is probably the most reliable means of calculating inclined pressure drop. The liquid head factor is used in conjunction with a horizontal two-phase correlation to estimate the total pressure drop through the pipe. The greatest error in using the Flanigan curve appears with high liquid mass velocities (above 66,000 #/hr-ft^2 for the system studied).

Shut-in data are presented which show the effects of incline and fluid flow rates on the amount of liquid in-place in the pipe.

High speed color films with informational titles are available at the School of Chemical Engineering, University of Oklahoma.

TABLE 11

NOMENCLATURE

F - refers to a "function of."

P - pressure, # Force/ft^2.

L - length of pipe, ft.

ϕ - Martinelli correlation parameter, function of X.

X - Martinelli et al., correlation, $= [(\Delta P/\Delta L)_l/(\Delta P/\Delta L)_g]^{1/2}$

$\left(\frac{\Delta P}{\Delta L}\right)_g$ - Martinelli correlation; pressure drop for gas phase, calculated as if gas were flowing alone in pipe.

$\left(\frac{\Delta P}{\Delta L}\right)_l$ - Martinelli correlation; pressure drop for liquid phase, calculated as if liquid were flowing alone in pipe.

D - pipe diameter, ft.

W - fluid flow rate, # mass/time.

A - pipe cross sectional area, ft^2.

ρ - density, # mass/ft^3.

μ - viscosity, # mass/ft-hr.

Re - Reynold's Number, dimensionless.

H - relative increase in pressure drop due to liquid holdup, dimensionless.

R - relative increase in pressure drop due to wave roughness, dimensionless.

f'_g - Schneider correlation, gas friction factor, dimensionless.

$$f'_g = \frac{\left(\frac{\Delta P}{\Delta L}\right)_{TP} \; g D \rho_g}{2 G_g^2}$$

TABLE 11 (Continued)

f_w - White correlation, friction factor, ~~dimensionless~~

$$f_w = \frac{2\, g_c\, D^6\, \Delta P_{TP}\, \rho_l}{L \left(\frac{W_l^{3.6}}{W_l + W_g}\right)}$$

ϕ_w - White correlation, flow modulus.

$$\phi_w = \left(\frac{W_l}{W_g}\right)^{1.8} \left(\frac{\rho_g}{\rho_l}\right)^{.9} \left(\frac{1}{\mu_g{}^{.1}}\right) \left(\frac{1}{\mu_l{}^{.1}}\right)$$

FR - flowing ratio, ft^3 air flowing/ft^3 liquid flowing.

SIR - shut-in ratio, ft^3 air in-place/ft^3 liquid in-place.

G - mass flow rate, # mass/hr-ft^2.

V - superficial velocity based on total pipe area, ft/unit time.

fm - Moody friction factor, dimensionless

$$fm = \frac{2\, g_c\, D\, \Delta P}{V^2\, \rho\, L}$$

Flow Pattern Nomenclature

R - ripple flow

W - wave flow

S - slug flow

C - cresting flow

SA - semi-annular flow

S-SA - combination of slug and semi-annular flow, hyphen between symbols denotes a combined flow type

Subscripts

l - refers to liquid phase

g - refers to gas phase

TABLE 11 (Continued)

TP	- refers to two-phase flow
G-O	- refers to gas-oil phase
Air	- refers to air phase
H_2O	- refers to water phase
avg	- designates an average reading

BIBLIOGRAPHY

1. Allen, W. F. "Flow of Flashing Mixture of Water and Steam through Pipes and Valves," Transactions ASME, 75, 1951, pp. 257.

2. Alves, G. E. "Co-current Liquid-Gas Flow in a Pipeline Contactor," Chemical Engineering Progress, 50, 1954, p. 449.

3. Baker, Ovid. "Design of Pipelines for the Simultaneous Flow of Oil and Gas," Oil and Gas Journal, July 26, 1954.

4. Baker, Ovid. "Speed-Up Flow Calculations for Design of Gas Gathering Systems," Oil and Gas Journal, May 16, 1955.

5. Bergelin, O. P., and C. Gazley, Jr. "Co-current Gas-Liquid Flow--I--Flow in Horizontal Tubes," Heat Transfer and Fluid Mechanics Institute, Berkley, Calif., Meeting, (Published by ASME), 1949, pp. 5-18.

6. Bergelin, O. P., P. K. Kegel, F. G. Carpenter, and Carl Gazley, Jr. "Co-current Gas Flow in Vertical Tubes," Heat Transfer and Fluid Mechanics Institute, Berkley, Calif., 1949, pp. 19-28.

7. Berry, A. L. and B. L. Moreau. "The Peace River and Alaska Highway Gas Gathering System," The Engineering Journal, November 1957.

8. Bertuzzi, A. F., M. R. Tek, and F. H. Poettmann. "Simultaneous Flow of Liquid and Gas Through Horizontal Pipe," AIME Transactions, 207, 1956, p. 17; Journal of Petroleum Technology, 8, January, 1956, p. 4,203.

9. Brigham, W. E., Holstein, E. D. and R. L. Huntington. "How Uphill and Downhill Flow Effect Pressure Drop in Pipelines Through Hilly Country," Oil and Gas Journal, November 11, 1957.

10. Brown, G. G. Unit Operations. New York: John Wiley & Sons, Inc., 1951.

11. Chenoweth, J. M. and M. W. Martin. "A Pressure Drop Correlation for Turbulent Two-Phase Flow of Gas-Liquid Mixtures in Horizontal Pipe," Petroleum Refiner, October, 1955, p. 151.

12. Flanigan, Orin. "Effect of Uphill Flow on Pressure Drop in Design of Two-Phase Gathering Systems," Oil and Gas Journal, March 10, 1958.

13. Galegar, W. C., R. L. Huntington, and W. B. Stovall. "Some Aspects of Vertical Two-Phase Flow," Petroleum Refiner, November, 1954.

14. Gazley, Carl. "Co-current Gas-Liquid Flow III. Interfacial Shear and Stability," Heat Transfer and Fluid Mechanics Institute, Berkley, Calif., 1949 (Available from ASME).

15. Gosline, J. E. "Experiments on the Vertical Flow of Gas-Liquid Mixtures in Glass Pipes," Transactions ASME, 118, 1936, pp. 57-70.

16. Holmes. "Flooding Velocities in Empty Vertical Tubes," Perry's Chemical Engineers' Handbook. McGraw-Hill, Figs. 17 and 18, p. 686.

17. Jenkins, R. "Two-Phase, Two-Component Flow of Air and Water," M.S. Thesis, University of Delaware, 1947.

18. Lockhart, R. W. and R. C. Martinelli. "Proposed Correlation of Data for Isothermal Two-Phase, Two-Component Flow in Pipes," Chemical Engineering Progress, 66, 1944, p. 139.

19. Lockhart, R. W. and R. C. Martinelli. "Proposed Correlation of Data for Isothermal Two-Phase, Two-Component Flow in Pipes," Chemical Engineering Progress, 45, 1949, p. 39.

20. Poettman, R. H. and P. G. Carpenter. "Multiphase Flow of Gas, Oil, Water through Vertical Flow Strings," Paper #851-26-I, Mid-Continent District API, Division of Production, March, 1952.

21. Schneider, F. N. M. S. Thesis, University of Oklahoma, 1951.

22. VanWingen, N. "Pressure Drop for Oil-Gas Mixtures in Horizontal Flow Lines," World Oil, 129, 1949, p. 156.

23. Versluys, J. "Mathematical Development of the Theory of Flowing oil Wells," Transactions AIME, 86, (Petroleum Development and Technology), 1930, p. 192.

24. White, P. D. Ph.D. Thesis, University of Oklahoma, 1952.

25. White, P. D. and R. L. Huntington. "Horizontal Co-current Two-Phase Flow of Fluids in Pipe Lines," The Petroleum Engineer, August, 1955, p. D-40.

APPENDIX I

SAMPLE CALCULATIONS

1. White Correlation
   Run No. 269

$G_{Air} = 4900$ lb. mass/hr-ft^2

$G_{G-O} = 3370$ lb. mass/hr-ft^2

$\rho_{Air} = .0716$ lb. mass/ft^3

$\rho_{G-O} = 51.5$ lb. mass/ft^3

$\frac{\Delta P}{\Delta L} = .085$ lb. force/ft^2-ft

$W_l = 82.5$ lb. mass/hr

$W_g = 120$ lb. mass/hr

$D = .1768$ ft

$$f_w = \frac{2\, g_c\, D^6\, \Delta P\, \rho_l}{L \left(\frac{W_l^{3.6}}{W_l + W_g}\right)}$$

$$f_w = \frac{2\,(32.2 \times 3600^2)\,(.1768)^6\,(.085)\,51.5}{\left[\frac{(82.5)^{3.6}}{82.5 + 120}\right]}$$

$f_w = 2.84$

$$\phi = \left(\frac{G_l}{G_g}\right)^{1.8} \left(\frac{\rho_g}{\rho_l}\right)^{.9} \left(\frac{1}{\mu_g{}^{.1}}\right) \left(\frac{1}{\mu_l{}^{.1}}\right)$$

$$\phi = \left(\frac{3370}{4900}\right)^{1.8} \left(\frac{.0716}{51.5}\right)^{.9} \left(\frac{1}{(.0436)^{.1}}\right) \left(\frac{1}{(7.98)^{.1}}\right)$$

$$\phi = .00152$$

2. Flanigan Correlation
   Run No. 279 - 2.3° Incline

G_{Air} = 3460 lb. mass/hr-ft^2

G_l = 89,200 lb. mass/hr-ft^2

$$V\left(\frac{ft}{sec}\right) = \frac{G_g \text{ lb} \quad \text{hr} \quad ft^3}{\text{hr-ft}^2 \times 3600 \text{ sec} \quad \rho_g \text{ lb}}$$

V = 13.0 ft/sec

$$\text{Liquid Head Factor} = 100 \times \frac{\Delta P_{TP} \text{ (inclined flow)} - \Delta P_{TP} \text{ (horz)}}{\rho_l \times h}$$

ΔP_{TP} (inclined) = .523 lb. force/ft^2 - ft

ΔP_{TP} (horz) = .250 lb. force/ft^2 - ft (From Fig. 7)

$$\text{Liquid Head Factor} = \frac{(.523 - .250) \text{ lb/ft}^2 - \text{ft}}{51.5 \text{ lb/ft}^3 \quad 1.12 \text{ ft}} \times 59.6 \text{ ft}$$

Liquid Head Factor = 28.0%

3. Air Friction Factor (Single Phase)
   Run No. A

$$f = \frac{2 \quad g_c \quad D \quad \Delta P}{y^2 \quad L \quad \rho}$$

V = 83,700 ft/hr D = .1768 ft

ρ = .0686 lb.mass/ft^3 μ = .0441 lb.mass/ft-hr

$\frac{\Delta P}{L}$ = .0773 lb.force/ft^2-ft

$$f = \frac{2 \times \left[32.2 \times (3600)^2\right] .1768 \quad .0773}{.0686 \quad (83700)^2}$$

f = .02365

Re = $DV\rho/\mu$

$$Re = \frac{.1768 \quad 83,700 \quad .0686}{.0441}$$

RE = 2.30×10^4

4. Per Cent of 2-Phase ΔP Due to Reduced Area For Air Flow
Run No. 160 - Angle of Incline - 0°

$$\%\ \Delta P \text{ increase} = \frac{\Delta P_{RA} - \Delta P_{1\ Phase}}{\Delta P_{2\ Phase} - \Delta P_{1\ Phase}} \times 100$$ (see pg. 63)

G_l = 29,100 lb.mass/hr-ft^2

G_g = 17,100 lb.mass/hr-ft^2

SIR = 25.1 ft^{3}air/ ft^{3}liq (in place)

FR = 424 ft^3 air/ft^{3}liq (flowing)

Flow Type - Semi-Annular
Vol available for air flow = 1.431 ft^3 (From Shut-In Data)

Reduced D = .1735 ft

Reduced Re = 7.0 10^4

f (reduced) = .023 (From Fig. 21)

μ_g = .0441 lb.mass/ft-hr

ρ_g = .0702 lb.mass/ft^3

$V_g = 247,000$ ft/hr

$$\frac{\Delta P_{RA}}{L} = \frac{f \; V^2 \; \rho}{2 \; gc \; D}$$

$$\frac{\Delta P_{RA}}{L} = \frac{.023 \; (247,000)^2 \quad .0702}{2 \quad 32.2 \quad (3600)^2 \quad .1735}$$

$$\frac{\Delta P_{RA}}{L} = .68 \text{ lb.force/ft}^2 - \text{ft}$$

$\Delta P_{1 \text{ Phase}} = .665$ lb.force/ft^2 - ft

$\Delta P_{TP} = 1.57$ lb.force/ft^2 - ft

$$\%\ \Delta P_{\text{increase}} = 100 \; \frac{.680 - .665}{1.60 - .665} = 1.60\%$$